AALBORG UNIVERSITY
STUDENT REPORT

Karl Eide Pollestad,

Protection of Permanently Shunt-compensated HVAC Cables

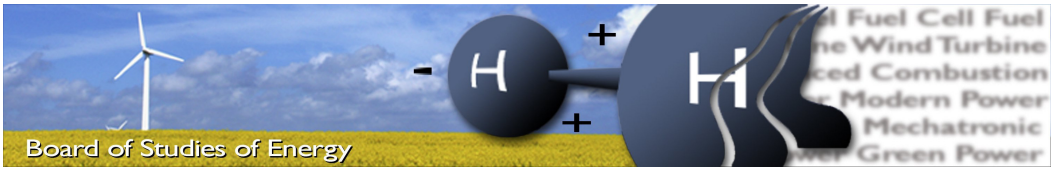

Title:	I Protection of Permanently Shunt-compensated HVAC Cable
Semester:	10^{th}
Project period:	01.02.14 to 03.06.14
ECTS:	30
Supervisor:	Claus Leth Bak
	Filipe Faria da Silva

Karl Eide Pollestad

SYNOPSIS:

This report describes the protection of a cable, compensated by a permanently connected shunt reactor. A current zero-missing is present for several seconds when the cable is energized at zero voltage and will pose a danger for the circuit breakers if they try to operate. A model is created in the transient software PSCAD to simulate different fault scenarios. The solution strategy is implemented in the relay using Digsi 4 software. The objective for this thesis is to improve the protection scheme by taking zero-missing into consideration.

Copies:	3
Pages, total:	75
Appendix:	2

Preface

This M.Sc thesis concludes my Master of Science education in Energy Engineering with specialization in Electrical Power Systems and High Voltage Engineering at Aalborg University. The thesis was performed in 2014 at the Department of Energy Technology, in collaboration with Energinet.dk.

Reading Instructions

- Figures are numbered sequentially in their own chapter. For example Figure 1.3 is the third figure in the first chapter.
- Equations are numbered in the same way as figures but they are shown in brackets.
- References are specified in the text in square parentheses according to Harvard method. The bibliography is on page 69.

Acknowledgements

The author of this report would like to thank Claus Leth Bak and Filipe Faria Da Silva for excellent guidance as supervisors for this thesis. Also a thank to Bjarne Bukh (energinet.dk) for creating the proposal for this thesis and Kasper Schultz Pedersen (energinet.dk) for providing the necessary data.

Contents

Chapter 1

Introduction

The focus of this master thesis is to gain understanding of issues regarding protection of long HVAC cables and transient phenomenon's like zero-missing. More precisely, the focus is to develop a protection scheme were both primary and secondary protection handle zero-missing phenomena.

1.1 Background

Overhead lines (OHL) have been for more than a century the most common used technology for transmitting electrical power over distances [5]. The use of HVAC cables have been mostly limited to densely populated areas until recently when their use in transmission networks have dramatically increased. The increase of underground cable transmission is very clear in Denmark, the first country in the world undergrounding most of its transmission network [6]. The danish government decided in 2008 that all transmission lines at 150kV level and below to be replaced by underground cables within the next 20 years. The plan also states that the danish transmission grid operator (TSO), Energinet.dk should build underground cables exclusively when planning new transmission lines at 400 kV level [6]. The plan as of 2032 is shown in figure 1.1

Some of the electrical characteristics of an transmission line are depending on the physical distance between the phases, the greater the distance the greater the inductance and smaller the capacitance. A cable differs from an OHL in the way that the phases are bonded much closer together. A great deal of the total capacitance is the capacitance to ground which does not depend on the distance between phases. In a cable there is capacitance between the conductor and the screen which gives the cable 10-20 times larger capacitance compared to an OHL [5]. The large capacitance leads to large generation of reactive power by the cable that needs to be consumed to prevent voltage rise and/or reduced transmission capacity of the cable. A reactor connected in shunt shown in figure 1.2 is commonly used in order to draw inductive current from the system and hence compensate for the capacitive current drawn by the cable.

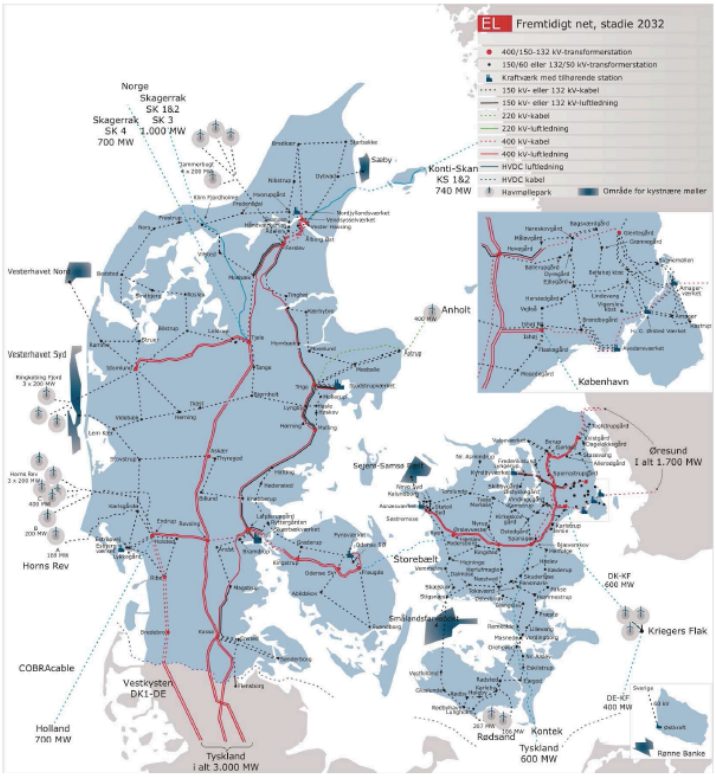

Figure 1.1: Cableplan of Denmark as of 2032 [19]

During the energization of cable and reactor there can be produced a dc-offset in the current of the circuit breaker (CB), so that it does not cross zero ampere for several cycles. This phenomenon is referred to as zero miss. In the event of a fault during this period, the circuit breaker for all three phases will operate but only the breaker for the faulted phase will successfully interrupt. The operation of the CB's for the two remaining phases will result in an arc for a prolonged period of time due to the dc current and hence damage the breakers.

Countermeasures to avoid zero-missing has been proposed in [4], [2] and [5]. This thesis will focus on how the protection relay can handle zero miss if it is present. In the case where the primary protection malfunction, a secondary protection relay would operate as backup protection. It is important that zero-missing phenomenon is taken into consideration for the design of the backup protection to prevent damage

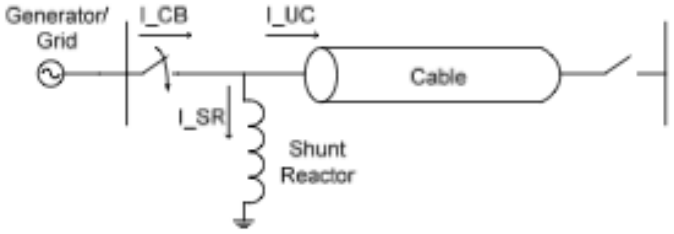

Figure 1.2: Single line diagram for CB, shunt reactor and cable [4]

to its CBs.

1.2 Thesis outline

Chapter 2 presents the system description which explains the most important components in the network under study.

Chapter 3 presents the problem analysis consisting off theoretical background and a thorough analysis of the problem. This chapter also presents a detailed problem statement

Chapter 4 presents The system modeling into EMTD/PSCAD.

Chapter 5 shows simulations for different faults and provides the results to be used as input to the relay

Chapter 6 presents the problem solving. It shows different proposed solution strategies within the boundary of the problem statement. The different strategies are examined in order to find the most suitable solution to implement

Chapter 7 presents the implementation of the solution strategies into the Software Digsi 4.

Chapter 8 presents the results from the testing done in the power system protection lab

Chapter 9 presents the conclusion and future work.

1.3 Initial problem formulation

It is necessary to develop a solution to avoid or handle zero-miss in the event of an unbalanced fault when energizing a cable with a permanently connected shunt reactor utilizing 100% compensation. It is important to detect zero miss and control the circuit breaker in order not to open the phases where zero miss is present.

Chapter 2

System description

2.1 Geography

The system under consideration in this report is the cable connection in Indkildedalen between Skudshale and Gistrup in north Jutland, Denmark. More precisely the cable is a 400 kV, 8,6 km that connects the stations FER and VHA as shown in figure 2.1. The cable on the HV line between FER and VHA will replace the existing overhead line which will be removed by the end of 2015.

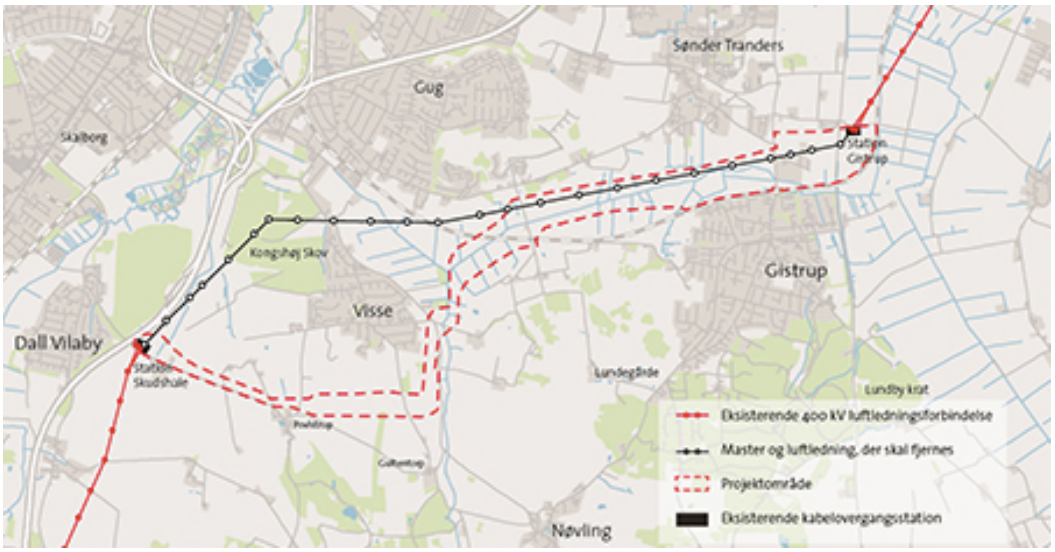

Figure 2.1: Skudshale-Gistrup

2.2 Cable

The cable planned to be installed is a 2000mm^2 AL XLPE 400KV Silec cable that will stretch from substation SKH trough Indkildedalen to substation GST. The

cable is laid in flat formation at a depth of 1.4 m below ground. The cables are cross-bonded in link boxes every 1.43 km. A drawing of the cable and its different layers is shown in figure 2.2 with the data for the layers is shown in table 2.1.

Figure 2.2: Drawing of the cable [1]

Cable drawing		
Layer	**Parametres**	**Values**
1:Conductor/Segmental/Watertight	Cross-section Material: Aluminium Indicative diameter	2000 mm^2 55.4 mm
2: Water blocking tape		
3: Inner semi-conductive layer	Indicative thickness	2mm
4: Insulation	Material: cross-linked polyethylene Minimum average thickness	 27 mm
5: Smooth outer semi-conductive layer	Indicative thickness	1.5 mm
6: Water blocking tape		
7: Metallic tape	Material: Aluminium stuck onto the outer sheeth, Inducative thickness	0.8 mm
8: Smooth outer sheet and extruded semi conductive layer	Material: High density polyethylene Minimum average thickness Indicative external diameter (D) Indicative weight	 0.8 mm 136 mm 17.3 kg/m

Table 2.1: Data for the different layers for the cable [1]

Cable Electrical features	
parametres	**Values**
Voltage level U0/U (Um)	230/400 (422) kV
Maximum conductor restistance in d.c. at 20 degrees	0.0149 ohm/km
Conductor resistance in a.c at 50 Hz, at 90 degrees	0.0193 ohm/km
Cable capasitance	0.203 μF/km
Conductor impedance	0.63 mH/km
K_s for 2000mm^2 Alu	0.19
K_p for 2000mm^2 Alu	0.37

Table 2.2: Data for the HVAC cable [1]

were:
K_s is a constancy used in the formula to calculate the skin effect of the cable
K_p is a constancy used in the formula to calculate the proximity effect of the cable

2.2.1 Cross bonding

Cross bonding is a common type of screen bonding in which, each screen circuit contains one section from each phase as shown in figure 2.3. The total voltage in each screen circuit sums to zero and if the screens are then bounded and earthed at the end, the net voltage in the loop and the circulating current will be ideally zero in balanced operation [35]. Due to practical considerations like cable length and laying conditions, there will always be a small residual voltage and a negligible current.

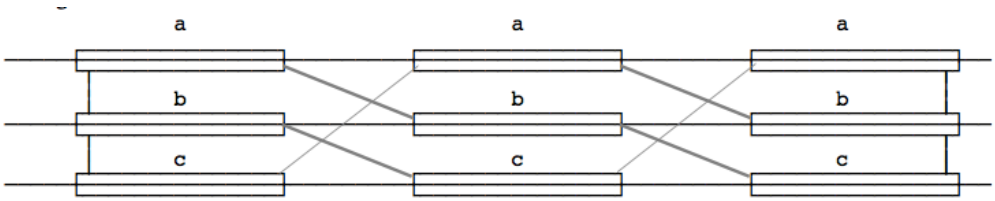

Figure 2.3: Cross bonding of cable screens [34]

3 minor sections make up one major section where the screen are solidly bonded together and to earth [34]. The screens are transposed between each minor section and the minor sections needs to be similar in length in order to make the system as balanced as possible [5]. The circulating current can be reduced and hence the current rating of the cable increased by the use of cross bonding of the cable.

2.3 Shunt reactor

The reactor installed at Indkildedalen is a 50-110 MVAR, 400 kV variable shunt reactor from ABB shown if figure 2.4. The shunt reactor is a 3-phase, five limb reactor with on-load tap changer. In order to reduce noise levels, the shunt reactor has been fittet with sound panels.

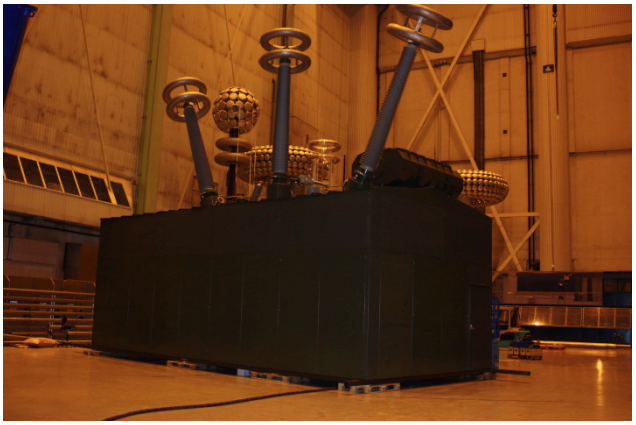

Figure 2.4: 50-110 MVA(R) Shunt reactor

The rating of the shunt reactor is shown in table 2.3.

Ratings	
Parameters	**Values**
Type of cooling	ONAN
Rating	50-110 Mvar
Rated voltage	400 kV
Max operating voltage	420 kV
Rated current	72.2-158.8 A
Insulation level	LI 1425 kV
	SI 1050 kV

Table 2.3: Data from the rating plate of the shunt reactor

2.4 Overhead line

North and south of the cable under study in this report, there is adjoining overhead lines. It is assumed that the cable will be energized at no load from FER and therefore it is not necessary to include the overhead line north of Indkildedalen. The 3.84 km distance between substation FER and SKH is divided into two OHL segments, 1.81 km and 2.03 km, respectively. The ohl's for the two distances have the same specifications and data for the phase lines and ground wires are shown in table 2.4.

Overhead line conductors		
Conductors	**Parameters**	**Values**
Phase wires	Tower	D11
	Name	772 SA
	Type	Martin Duplex
	Outer radius	0.018085 m
	Total number of strands	54
	Number of outer strands	24
	Strands radius	0.00201 m
	DC resistance	0.04227 Ω/km
Ground wires	Tower	D11
	Name	153 SA
	Type	Dorking
	Outer radius	0.008 m
	DC resistance	0.299 Ω/km

Table 2.4: Martin type phase wires and Dorking type ground wires

2.5 Relays

At 400 kV transmission level there will always be two main protections relays, mains 1 and mains 2. At Indkildedalen the two relays are SIPROTEC 4 line differential and distance protection 7SD522 and Line distance protection REL670 shown in figure 2.5. The relays are delivered by Siemens and ABB, respectively.

(a) Mains 1: SIPROTEC 4 7SD522, Siemens **(b)** Mains 2: REL670, ABB

Figure 2.5: The two main protection relays

2.5.1 Line differential and distance protection, SIPROTEC 4 7SD522

Siptrotec 4 7SD522 is a numerical protection relay that combines differential and distance protection. SIPROTEC 4 7SD522 holds a wide variety of protection features used in line protection. The differential protection functions of 7SD522 is used as main protection for Indkildedalen while the distance protection function is used as backup in case of communication loss etc.

2.5.2 Line distance protection, REL670

The line distance protection, REL670 belongs to the Relion®protection and control product family from ABB. The distance protection function of REL670 is used as primary protection and its overcurrent functions are used as secondary protection.

2.6 Circuit breakers

The circuit breakers planned to be installed at Indkildedalen are the 400 kV ABB LTB420 E2 which is a live tank circuit breaker from ABB shown in figure 2.6. The term live tank relates to the fact that the extinguishing medium and contacts are located at high voltage potential and hence "live". Other CB's with the breaker unit at ground potential are given the term "dead tank CB".

Figure 2.6: Live tank circuit breaker, ABB

The LTB420 is a Auto-Puffer™ based SF6 circuit breaker. One important feature of the auto-puffer design is the current-dependent build-up of extinguishing pressure [24]. As the contacts parts, there will be drawn an arc between the stationary and moving contact. The arc burning between the contacts will block the flow of SF6 gas trough the nozzles. The gas is heated by the arc and the pressure

inside the Auto-Puffer™ increase due to temperature as well as the compression of the gas between the puffer cylinder and stationary piston. As the current decrease towards zero crossing, the arc diameter also decreases, letting the pressurized gas flow trough the nozzle and extinguish the arc [22]. Figure 2.6 shows two breaking chambers in series mounted on an support insulatior and a support structure. The LTB420 has single pole mode capabilities which means that each phase can be switched individually by the means of ABB's Switchsync™ controller.

Chapter 3

Problem Analysis

The purpose of this chapter is to provide the reader with knowledge regarding the most important aspects leading to the final problem statement. The chapter also gives a guide to how this problem will be solved throughout this thesis.

During this chapter the reader will be provided with the relevant theory to fully grasp the problem and following solutions proposed. Why zero miss would be a problem seen from the circuit breaker perspective, how and why it is generated and how to counter zero missing phenomenon is initially explained. Different solution approaches will be presented through this section, leading to a final problem statement.

3.1 Circuit-breakers

It is important to understand why switching during current zero-miss will cause a problem to the circuit breakers. A circuit breaker is defined as an apparatus in electrical systems that has the capability to, in the shortest possible time, switch from being an ideal conductor to an ideal insulator and vise versa [20]. The most important task of a circuit breaker is to interrupt a fault current and hence protect electric components. In addition to interruptive functions, a CB is also applied for intentional switching such as energizing and de-energizing of shunt reactors etc [20].

There are several requirements that a circuit breaker should fulfill [21], [20]:

- In closed position the CB must be able to break the current without generating impermissible overvoltages
- In stationary closed position the CB should conduct its rated current without producing impermissible heat rise in any of its components
- In open position the CB must be able to switch on the current without the contacts being welded together

- In a stationary position, open or close, the circuit breaker must be able to withstand any over voltages within its rating

3.1.1 Mechanical and thermal stress imposed on a CB

A CB will be exposed to mechanical and thermal stress in closed position, but the biggest challenges lies in the breaking operation [21]. During a fault in the power grid, the fault current will run trough the CB until the fault has been disconnected. The mechanical forces during a fault is proportional with I^2, meaning a 20 kA fault will give 4 times the mechanical forces of a 10 kA fault [21].

The thermal strains on a CB is mostly caused by the rated current passing trough the CB during normal operation. When the contacts are parted mechanically there will be an arc between the contacts. The arc consist of extremely hot plasma which consists of a mix of positive and negative ions. The temperature in the arc is in the range of 5000-20000 degrees and the arc has a electric conductivity compared to that of carbon [22]. Only when the contacts are in virtually open position will the CB be capable of disconnection the current but only at the point of natural current zero crossing [21]. The cross-section of the arc is approximately proportional to the current and in the vicinity of current zero crossing, the arc has been cooled down to around 2000 degrees and it will no longer be ionized plasma, nor electrically conductive [22].

The current interrupting process is a complex matter that can be divided into two distinct regimes [24]:

- Thermal regime: At current zero crossing the arc channel must be rapidly cooled to a temperature were it is no longer conducting. When the current approaches zero, there is still a certain amount of electrical conductivity left in the arc path which gives rise to what is called a "post-arc-current". The success of the interruption depends on the race between the cooling and the energy input in the arc path by the transient recovery voltage (TRV). If the energy input exceeds the energy removal in the form of cooling, the breaker fails thermally.
- Dielectric regime: After having passed the thermal region, the voltage rises relatively fast at the CB terminals and the interruption is depending on the voltage withstand capability in the contact gap. The dielectric regime is located some hundreds of microseconds (depending on the CB) after zero crossing and at this time the CB has to withstand the full peak value of the TRV. The voltage withstand capabilities must be higher that the recovery voltage for the interruption to be successful.

Traditionally air and oil has been frequently used as insulation and extinguishing medium. Nowadays SF_6 gas has replaced air and oil as medium for economical and practical reasons, and also due to increased demand for higher ratings [20]. Compared to air, SF_6 has both a higher dielectric strength and better cooling capabilities. This means that SF_6 insulated breakers needs fewer breaker chambers in series compared to an air blast CB of similar rating. The SF_6 breaker is superior to the older types like oil and air blast CB and requires less maintenance [20].

Transient recovery voltage (TRV) can be calculated as follows [22]:

$$u_c = \frac{Ur * k_{pp} * \sqrt{2} * k_{af}}{\sqrt{3}} \tag{3.1}$$

where:
Ur= Rated voltage
k_{pp}= first pole to clear factor
k_{af}= Amplitude factor (1.4 of SCC according to IEC)

k_{pp} is depending on the earthing of the network [22]:

- k_{pp}=1.3 corresponds three-phase fault in a network with earthed neutral
- k_{pp}=1.5 corresponds three-phase fault in isolated and resonant earthed systems or unearthed systems
- k_{pp}=1.0 corresponds to special cases

3.1.2 Controlled switching

Random closing or opening of CB may lead to severe voltage and current switching transients. Energizing of shunt reactors, shunt capacitors and power transformers may cause transients like; Over voltages, Under voltages or inrush current [22]. Energizing a cable in parallel with a shunt reactor may cause a transient phenomenon called zero-missing phenomenon which is described in section 3.3.

The magnitude of the transients depends on the point on wave were the opening or closing of the CB contact occur. Controlled switching means that the instant of switching is controlled to occur on the most optimal point on wave to reduce or avoid harmful transients. In a 3-phase system, each phase must be controlled independently because of the 120 degree displacement of the voltages, so that the switching on each phase is done on the desired point on wave. More on controlled switching to reduce zero-missing is explained in section 3.4.

3.2 Shunt reactors

Cable lines becomes a source of reactive power due to the large capacitance within the cable. The production of reactive power needs to be consumed in order to avoid voltage rise in the cable and to avoid reactive power from flowing in the network. In order to understand why there can be a voltage rise in a cable we need to look at a phenomenon typically called Ferranti Effect. Using a two-port network for a medium length π-model, the sending voltage equals [7]:

$$V_s = (1 - \frac{YZ}{2})V_r + ZI_r \tag{3.2}$$

where: Y is the admittance Z is the impedance

The equation for calculating receiving end voltage for a lossless, unloaded line becomes; 3.3 [5]

$$V_r = V_s \frac{1}{1 - \frac{\omega^2 l^2 LC}{2}} \tag{3.3}$$

where:
L=$\frac{mH}{km}$
C=$\frac{\mu F}{km}$
l=km

Ferranti effect can also be explained on the basis of net reactive power flow in the line. If the reactive power generated at a point is more that what is absorbed, the voltage at that point becomes higher that its nominal voltage. Capacitance generates reactive power while inductance absorbs reactive power. Under light or no loading the capacitance of the line generates more reactive power than which is absorbed ad hence there will be a voltage rise [8]. Due to the larger capacitance the voltage rise will be greater in cables compared to OHL, but the effect will be present in both and will increase with the square of the length [5]. Cables has a 10-20 times higher capacitance than an overhead line (OHL) and ferranti effect is more pronounced in cables than OHL's [5]. Due to the lower capacitance, the length of the OHL must be longer than the cable before the ferranti effect is larger than the line losses and the voltage starts to increase

To compensate for the capacitance of the cable a shunt reactor is connected at the substation at Gistrup. A shunt reactor is defined by [16], as a reactor intended to be connected in shunt to an electric system for the purpose of drawing inductive current. The level of compensation is depending on the size of the inductor compared to the capacitive current in the cable. It is preferable to compensate for 100% of generated reactive power so that the reactive power balance in the grid is not affected by the cable line.

A shunt reactor is basically an RL circuit where the inductance is typically hundreds of times larger than the reactance. The current in a shunt reactor can therefore be calculated by [5]

$$I(t) \simeq \frac{V_p}{\sqrt{(R^2 + (wL)^2)}} (sin(wt + \theta - \frac{\pi}{2}) - sin(\theta - \frac{\pi}{2}) e^{-} \frac{Rt}{L}) \tag{3.4}$$

The current in equation 3.4 consists of two components:

- Steady-state component:
$$sin(wt + \theta - \frac{\pi}{2})$$
- Transient component:
$$sin(\theta - \frac{\pi}{2}) e^{-} \frac{Rt}{L}$$

The steady-state component is basically a sine wave approximately 90 degrees lagging the voltage. This part is not dependent on the switching instant as compared to the transient part. The transient component is a decaying DC amplitude whose initial amplitude depending on the switching instant.

For switching at peak voltage the DC component will be zero since θ becomes $\frac{\pi}{2}$. For switching at zero voltage the DC component will have the same initial magnitude as the AC component. This DC offset in the reactor current can have implications if the reactor is in parallel with a capacitance. That leads us to the next section, regarding zero-missing phenomenon.

3.3 Zero-missing phenomena

When a HVAC cable connection is energized with a shunt reactor, a DC-offset current can prevent the current trough the circuit breakers to cross zero [2][3]. This absence of zero crossing is referred to as zero-missing phenomena. Zero-missing phenomena can occur when the shunt reactors compensates for more than 50% reactive power generated from the cable. This phenomena can persist for several seconds depending on the rate of compensation and moment of switching [4] [5].

A single phase to ground fault occurring during the zero-missing period would lead to the following operation of the circuit breakers:

- The circuit breakers for all three phases will be sent a trip signal and the breakers will try to open their contacts
- The faulted phase would immediately succeed to disconnect
- The circuit breakers for the two healthy phases would not immediately interrupt due to the absence of current zero crossing which would cause an arc in the breaker chamber over an extended period of time

Zero-miss can put the circuit breakers under a lot of stress which may lead to breaker failure if they try to open their contacts during this period, unless they are designed for breaking DC current [3].

In order to explain the principle of zero-missing the cable+shunt circuit can be represented by an inductor in parallel with a capacitor. 100% reactive power compensation of a cable using a shunt reactor would be similar to a capacitor in parallel with an inductor of equal impedance. The current in the capacitor and the inductor would be of equal amplitude but in phase opposition to each other.

The voltage and current in an inductor is at 90 degrees phase difference, meaning if the voltage is zero the current is maximum and vice versa. The inductor would also have a DC component, who's initial magnitude can be as high as the peak magnitude of the AC current, depending of the voltage at the moment of connection. For switching at zero voltage the magnitude of the DC component would be equal to the peak magnitude of the AC component. This is because the current in an inductor, due to continuity must be continuous and hence zero before and right after energization, assuming there is no initial charge in the inductor. There would

be no DC offset when switching at peak voltage but this would lead to switching overvoltages and will therefore create new problems [5].

A shunt reactor in parallel with a cable can be seen as an parallel RLC-circuit. In order for a zero miss to be present the DC component must be larger or equal to the AC component of the current trough the CB shown in figure 3.1.

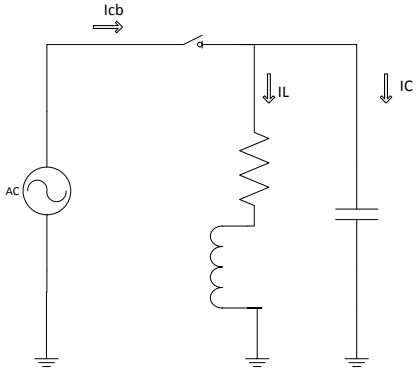

Figure 3.1: Basic RLC circuit

The current trough the circuit breaker of figure 3.1 can be calculated in time-domain by 3.5

$$I_{CB} = \frac{V_p}{R^2 + \omega L^2} sin(\omega t + \theta - tan^{-1}(\omega \frac{L}{R})) + C\frac{d(Vsin(\omega t))}{dt} \tag{3.5}$$

An alternative method of calculating the current trough the CB is to do the calculation in S-domain using Laplace Transforms. The total impedance consist of the resistance and inductance in series, and in parallel with the capacitance.

$$Z_{eq} = (\frac{1}{R + j\omega L} + \frac{1}{\frac{1}{j\omega C}})^{-1} = \frac{1}{\frac{1}{j\omega L + R} + j\omega C} \tag{3.6}$$

The equivalent impedance can be obtained in S-domain using Laplace Transform

$$Z_{eq} = (\frac{1}{R + sL} + \frac{1}{\frac{1}{sC}})^{-1} = \frac{1}{\frac{1}{Ls + R} + sC} \tag{3.7}$$

By defining the voltage as the input and the current as the output a transfer function G(s) can be obtained

$$Vi = I_{eq} * Z_{eq} -> G(s) = \frac{I_{eq}}{Vi} = \frac{1}{Z_{eq}} = \frac{CLs^2 + CRs + 1}{Ls + R} \tag{3.8}$$

$$Input = V_p * sin(\omega t + \pi) = -\frac{V_p \omega}{\omega^2 + s^2} \tag{3.9}$$

RLC values	
Parameters	**Values**
Voltage level V_P	400 kV
Resistance R	1.6 ohm
Capacitance C	1.7458 μF
Inductance L	5.8 H

Table 3.1: RLC line values assuming 100% compensation

By multiplying 3.8 and 3.9 in Laplace domain, the current trough the CB can be attained

$$I_{CB}(s) = -\frac{V_p\omega}{\omega^2 + s^2} * \frac{CLs^2 + CRs + 1}{Ls + R} \tag{3.10}$$

3.10 can be transferred back to time domain using inverse Laplace Transform, giving the equation 3.11

$$I_{CB}(t) = V_P(-\omega C cos(\omega t) + \frac{-Rsin(\omega t) + \omega L(cos(\omega t) - e^{-\frac{Rt}{L}})}{\omega^2 L^2 + R^2}) \tag{3.11}$$

By adding values for R,C and L the formula is more comprehensible. The capacitance of the cable is in μF/km and the length was given in section 2.2 in table 3.1

$$C = 0.203\mu F/km * 8.6km = 1.7458\mu F \tag{3.12}$$

Assuming 100% compensation, X_C=X_L and hence

$$L = \frac{1}{\omega^2 C} = 5.8H \tag{3.13}$$

With the given values equation 3.11 becomes the more straightforward equation 3.14:

$$I_{CB}(t) = -219.5e^{-\frac{1.6t}{5.8}} - 0.39cos(10\pi t) - 0.19sin(10\pi t) \tag{3.14}$$

where:
-$219.5e^{-0.27t}$ is the decaying DC-component
-0.39 cos(10π t)-0.19 sin(10π t) is the AC-component

The result is plotted in 3.2 as a function of time for the first 30 seconds after energization in order to show zero-miss. It is seen from figure 3.2 that there will be zero crossing approximately between 20-25 seconds after energization.

The exact instant of zero crossing is found solving for DC component+AC_{peak} component =0. This gives a result that the current reach zero 22.6 seconds after energization, which fits well with figure 3.2.

To get a more accurate model, the cable can be represented by its equivalent pi-model instead of just a simple capacitance as shown if figure 3.3. Here the shunt reactor is represented same as in figure 3.1, while the cable is represented by the

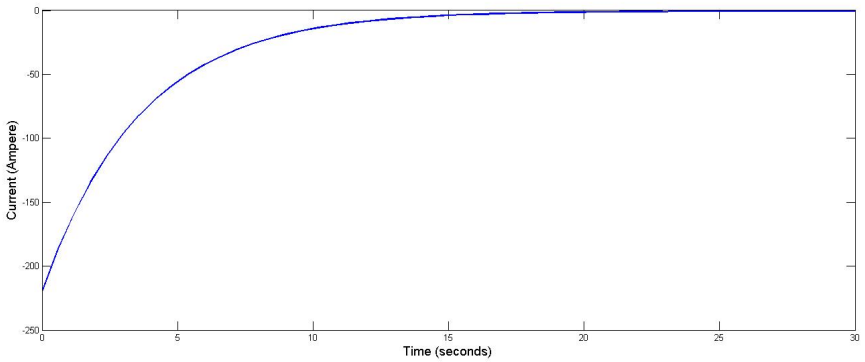

Figure 3.2: Zero-miss present in a RLC circuit assuming 100% reactor compensation at the start of the cable

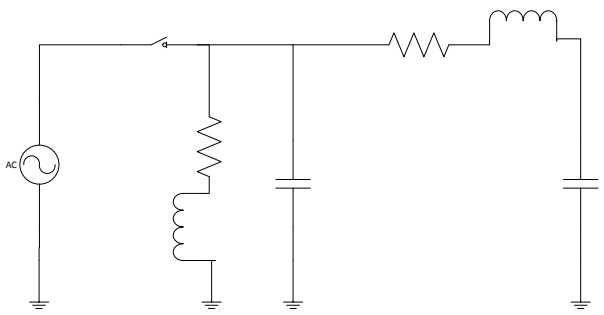

Figure 3.3: RL+PI-section used to represent shunt+cable

PI-branch consisting of an inductor in series with a resistor, in parallel with the capacitance.

The current trough the CB of the circuit of figure 3.3 is be calculated using PSCAD and the current shown in figure 3.4

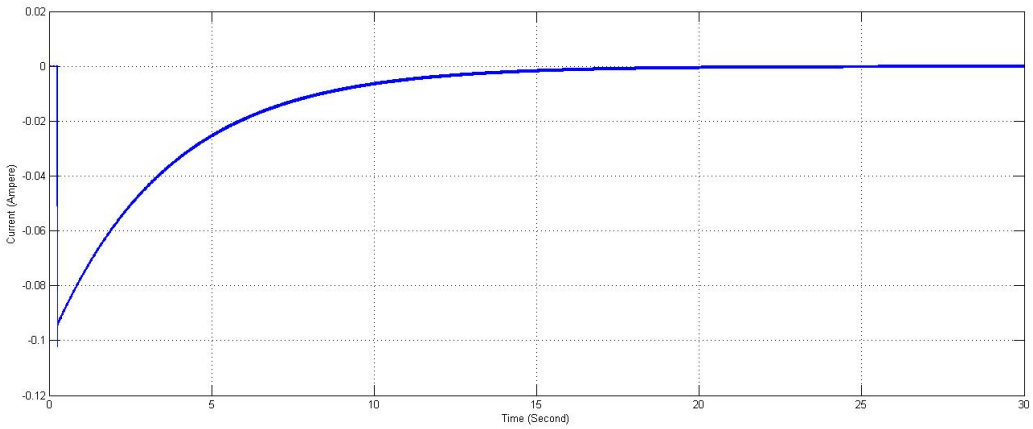

Figure 3.4: Zero-miss shown for 100% compensation using pi-section

It can be seen that the simulation using a PI-section to represent the cable greatly resembles the initial estimate using only a RLC representation shown in 3.2. If the goal is to only verify if zero-miss is present and its initial value, it is possible to simplify the calculations. Any resistance in the circuit will mainly decide how rapidly zero-miss would decay and the phase angle of the the inductive current. The phase shift due to the resistance will be very small and barely influence the initial value of the resulting CB current. The resistance will therefore not be considered during this calculation. As long as the DC component is larger or equal to the resulting AC component for the cable+shunt, there would be a zero-missing in the current through the circuit breaker. This means that we can start by calculating the current through the inductor (IL) and the current through the capacitor (IC). The current through the Inductor, IL is calculated by 3.15 and the current through the capacitor, IC is calculated by 3.16

$$IL = \frac{V}{\omega L} \tag{3.15}$$

$$IC = V\omega C \tag{3.16}$$

The current trough the CB will be the product of the inductive current and the capacitive current which is in phase opposition to each other. For switching at zero voltage the AC current of the capacitor and inductor would, assuming 100% compensation, cancel each other out leaving only the DC current as shown in figure 3.5. The decay time constant for this DC current depends on the resistance in the circuit.

Using the parameters from the cable and the shunt rector at Indkiledalen it is possible to prove that the DC component is larger than half of the the AC

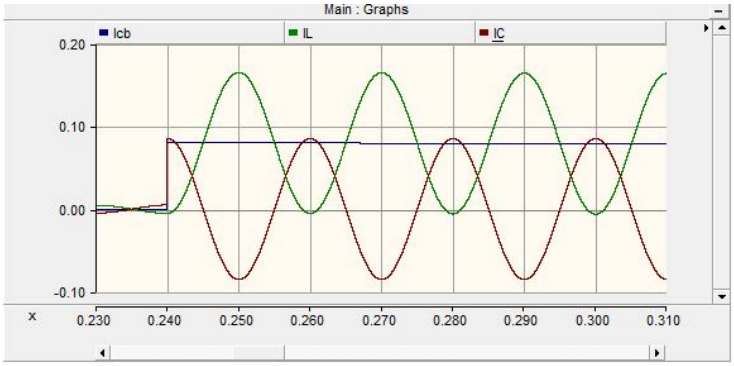

Figure 3.5: I_L and I_C cancel each other, leaving only a DC, hence Zero-miss is present

component and hence the existence of a zero-miss.

Using equation 3.15 and 3.16

$$I_C = 400kV * 2\pi * 50Hz * 1.7458\mu F = 219.4A \tag{3.17}$$

Assuming 100% compensation

$$I_L = \frac{400kV}{2\pi * 50Hz * 5.8H} = 219.4A \tag{3.18}$$

Since the inductor and capacitor current is in phase opposition, the AC current trough the CB is attained by subtracting the two current I_L and I_C, which will be zero.

DC component can be as high as the inductor current (I_L) depending on the switching instant. For switching at zero voltage, the initial value for the DC component and hence the current trough the CB would be 219.1 A. This fits well with the initial value calculated by equation 3.10 and shown in figure 3.2

Assuming 50% compensation, X_C=0.5*X_L and hence

$$L = \frac{1}{2 * \omega^2 C} = 11.61H \tag{3.19}$$

$$I_L = \frac{400kV}{2\pi * 50Hz * 11.61H} = 109.7A \tag{3.20}$$

It can be seen from equation 3.3 that for 50% compensation, the current trough the CB will touch zero during the first cycle due to the fact that the DC magnitude is exactly half of the AC-peak magnitude. Any higher rate of compensation would mean a higher inductor current, leading to a higher DC component and hence zero-miss.

Determining roughly the presence of zero-miss is possible depending on the time of switching using 3.15 and 3.16. Once it is verified that zero-miss is present it is interesting to know for how long. A formula for calculating the duration of zero-missing phenomenon for a shunt reactor connected at sending end of a cable was

presented in [5], shown in 3.21.

$$t = -\frac{Ls}{Rs} * ln|\frac{(x-1)}{(xcos\theta)}| \tag{3.21}$$

where:
x=compensation rate
θ= switching angle

A shunt reactor installed at receiving end would give a slightly shorter duration of zero-miss as a result of increased resistance for the current closing loop that now must go trough the cable [5].

Given 75% shunt compensation, equation 3.21 can tell us that the zero-miss will be present for

$$t = -\frac{3.87}{1.6} * ln|\frac{(0.75-1)}{(xcos(0))}| = 2.66s \tag{3.22}$$

This is also verified using PSCAD and shown in figure 3.6

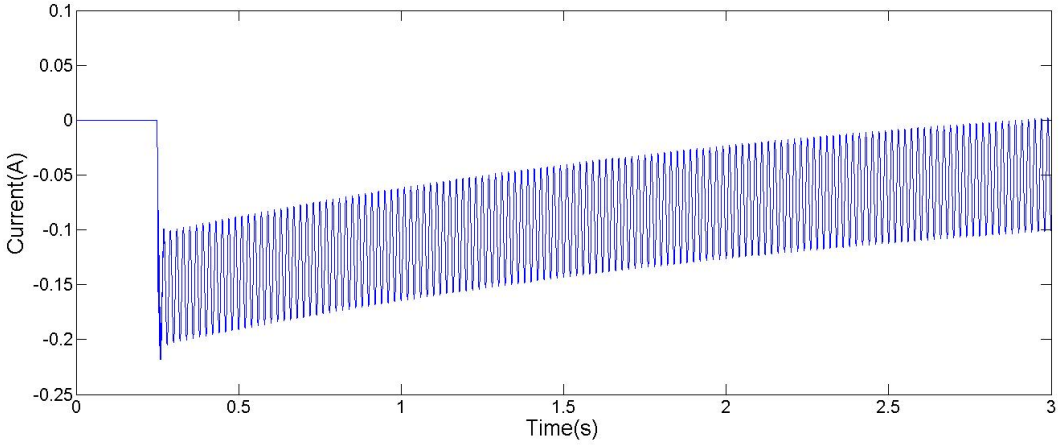

Figure 3.6: Zero-miss shown for 75% compensation

3.4 Countermeasures for zero-missing

3.4.1 Shunt reactor connected trough a CB

There has been developed several countermeasures to deal with zero-missing phenomena. The simplest countermeasure to avoid zero-missing would be to have the shunt reactor connected to the cable trough an additional circuit breaker. This configuration gives the possibilities to first connect the cable at zero voltage, then connect the shunt reactor at peak voltage, avoiding DC offset [5]. For this operation its required that the circuit breaker have synchronized switching capabilities.

During energization there will be a voltage swell due to the lack of compensation and therefore it is important to analyze that this does not violate the grid codes.

Regardless of a DC offset in the current trough the CB connecting the cable, there would always be zero crossing for the current in the shunt reactor, hence the shunt reactor can be disconnected. After the shunt reactors has been disconnected the inductor current is no longer present and the current trough the cables's CB only has an AC component. Therefore it is now possible to disconnect the cable [2].

The extra cost for an additional circuit breaker tends to make utility companies look for alternative solutions.

3.4.2 Controlled switching

3.4.2.1 Synchronous switching /Point on wave switching

A circuit breaker capable of switching the three phases independently is said to have synchronous/point on wave switching capabilities or single pole mode. When each phase of the cable it energized at its voltage peak the DC component can be minimized and thereby prevent zero-missing to occur. Synchronous switching is proven technology often applied to transformer energization to minimize inrush currents [6]. The drawback of this countermeasure is the extra investment required to purchase a circuit breaker with single pole mode. There is also the problem that the switching must be very accurate in order remove zero-missing when 100% compensation is applied. It was shown in [18] that during synchronized switching there could be a switching offset of 0,5 ms, which would lead to the presence of zero-missing and a DC current of 30 A when 100% compensation is applied [18]. It was therefore concluded in [18] that synchronized switching is not a viable solution due to the lack of precision.

3.4.2.2 Sequential switching

Sequential switching has a long record in applications for HVAC cable lines, and also requires circuit breakers with single pole mode [6]. A single phase fault would cause a large AC fault current running trough that phase. The current trough the circuit breaker on the faulted phase would have natural current zero crossing, hence the CB can interrupt. Since the fault has now been isolated, the CB on the healthy phases can wait some time before they break the line current [6]. If the shunt reactor is connected trough a CB, then the shunt reactor will be disconnected as the next step. Then the CB for the healthy phases at receiving end will disconnect and finally also the CB at sending end so that the CB for all phases has been opened.

The problem with switching the faulted line and then waiting for zero crossing before switching the two other phases is the possibility of ferroresonans. This phenomena is briefly explained in appendix B. If additional CB for the shunt reactor is installed this is avoided but this provides an extra cost explained earlier.

3.4.3 Pre-insertion resistor

Another possibility for removing zero miss is by the use of a pre-insertion resistor. Pre-insertion resistors have traditionally been used to reduce voltage transients when energizing no-load transmission lines. In many cases controlled switching has replaced pre-insertion resistors due to better switching properties of new circuit breakers [20]. A pre-insertion resistor consists of a resistor in parallel with the breaking chamber of the CB. The resistor will close the circuit 8-12 ms prior to the arching contacts and therefore damp the DC current and reduce the time zero miss is present [5]. Pre-insertion resistors can according to [4] be an important countermeasure for zero-miss as the added resistance will damp the DC component quickly if the value of the resistor is well designed. A pre-insertion resistor also has the advantage that any over-voltages would also be damped.

The value of the pre-insertion resistor is of great importance and needs to be calculated. If the value is to small it will not be able to damp the entire DC component in the given time of 8-12 ms. If the resistor is to large, it will be equivalent to an open source and bypassed [5].

The procedure for calculating the value of the pre-insertion resistor is shown in [4] and [5]. The pre-insertion resistor required for Indkiledalen would have the value of 1210 ohm [18].

Energinet choose not to instal Pre-insertion resistors in Indkiledalen due to the cost of this installation on the CB's as there does not exist any standard resistor sizes for this value [18].

3.4.4 Variable reactor

By reducing the compensation rate to 50% while energizing, zero missing phenomenon can be avoided. This require more expensive shunt reactors and there is a risk of high voltage disturbances, as the voltage may exceed operational limits during energization [25]. For Indkiledale, energinet.dk has calculated that the voltage swell would not exceed the 3% limit [18]. Variable reactor is a solution used in Denmark previously and is also the current planned solution for Indkiledalen. The extra cost of a variable reactor along with voltage swell during energization makes this solution not ideal and hence it would be beneficial to develop new methods that allows for a higher rate of compensation during energization.

3.5 Protection of HVAC cables

Electric cables are designed to operate below a certain temperature called the cables thermal withstand limit. The thermal withstand limit depends on conductor material and insulation type and thickness [15].

Underground cables must be protected agains excessive heat created during a fault and the fault must be cleared before the cable reaches its thermal withstand limit. The heating of the cable is depending of the fault current and time it takes for the fault to be cleared Thermal heat generated in the cable is proportional

with I^2t. The cost of a HVAC cable installation is several times higher than of an equivalent overhead line. Locating and performing repairs on an underground cable system may take days or weeks [10].

The demand for quick fault clearance in HVAC cables has resulted in the practice of using unit protection. Unit protection provides independent protection for the protected circuit and isolates fault at higher speed. The downside of using unit protection is higher cost of relays and the cost related to any communication devices that are needed. Differential protection relays are often used as main protection for HVAC cables and the backup protection usually adopts some distance protection scheme.

3.5.1 Differential Protection

One form of unit protection often applied in feeder protection is also known as differential protection, as the principle is to sense the difference in current of the incoming and outgoing terminals of the protected circuit [11]. The principle of differential protection was first established by Merz and prize at the beginning of the 20th century [12].

The most fundamental type of differential protection is the circulating current system shown in fig 3.7. These relays are frequently used and the function is straightforward in principle. Under load current and external fault current, the current entering and leaving the terminals of the protected circuit is equal assuming ideal CTs. Under external faults or load current, the current from the CTs at the two terminals would be circulating the same direction and there will be no current running trough the differential measuring branch where the relay is located. During an internal fault, the current will flow towards the protective device from both ends and the circulating current would go trough the differential branch, tripping the relay. Current differential principles are not dependent on cable characteristics and is therefore the most sensitive and reliable protection scheme for cables [17].

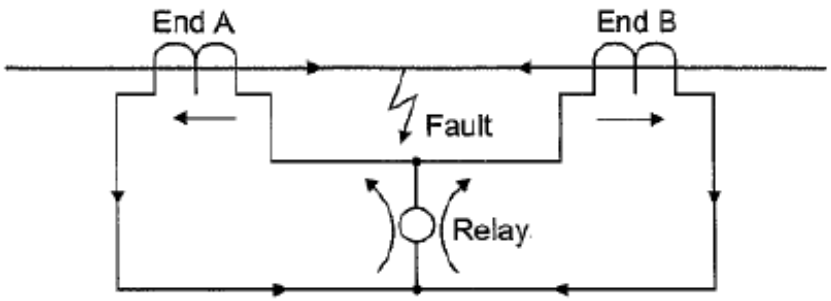

Figure 3.7: Basic principle off a Differential relay

3.5.2 Distance Protection

Distance protection in its basics is a non-unit protection which has several economic and technical advantages. Distance protection is simple to apply and can provide both primary and backup protection. When adapted with a signaling channel between two relays, distance protection satisfies the criteria for a unit protection scheme. The basic principle of distance protection is based on dividing the voltage at the relaying point by the measured current [11]. The impedance is then compared to the reach point impedance. If the measured impedance is less than the impedance calculated for the reach point, it means that a fault is present between the relay and the reach point [14]. To improve selectivity each line plus adjacent lines are divided into several segments with a protection zone dedicated to each segment as shown in figure 3.8. To ensure selectivity there is a time grading separating trip signals depending on which zone the fault is located.

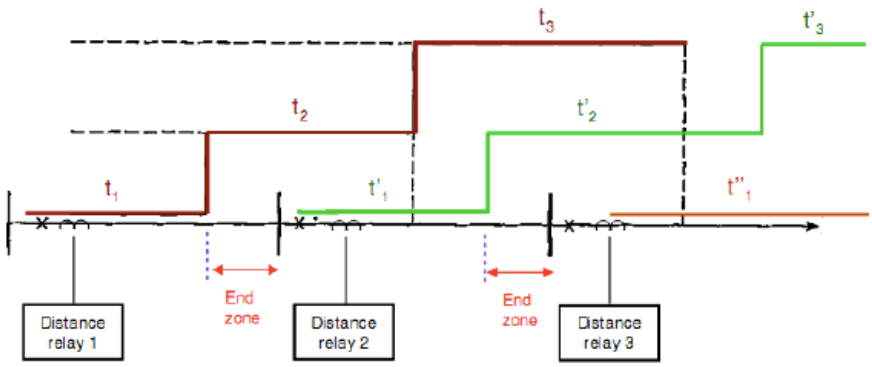

Figure 3.8: Basic principle off a Distance relay, graded distance zones [14]

3.5.3 Numerical Protection Relays

Late 1980 with the introduction of microprocessors, numerical technology was introduced to protection applications. Numerical relays use one or more digital signal processors optimized for real time signal processing, running the mathematical algorithms for the protection functions [11].These modern relays are multi-functional capable of executing additional tasks such as operational measurements and disturbance recording. Self monitoring replace the necessity of costly preventive routine maintenance with event driven maintenance [26].

Numerical relays has the functionality that previously required several relays, hence protection functions such as differential protection and distance protection are now referred to as "relay elements". Each relay element is in software so that the signal processor can run a vast variety of relay elements [11]. Numerical devices may be operated both locally and remote with a PC via remote serial interface.

Hardware Architecture of Numerical Relays The typical architecture of a numerical relay is shown in figure 3.9. The relay consists of digital signal processors, memory, digital and analog input/output and power supply [11].

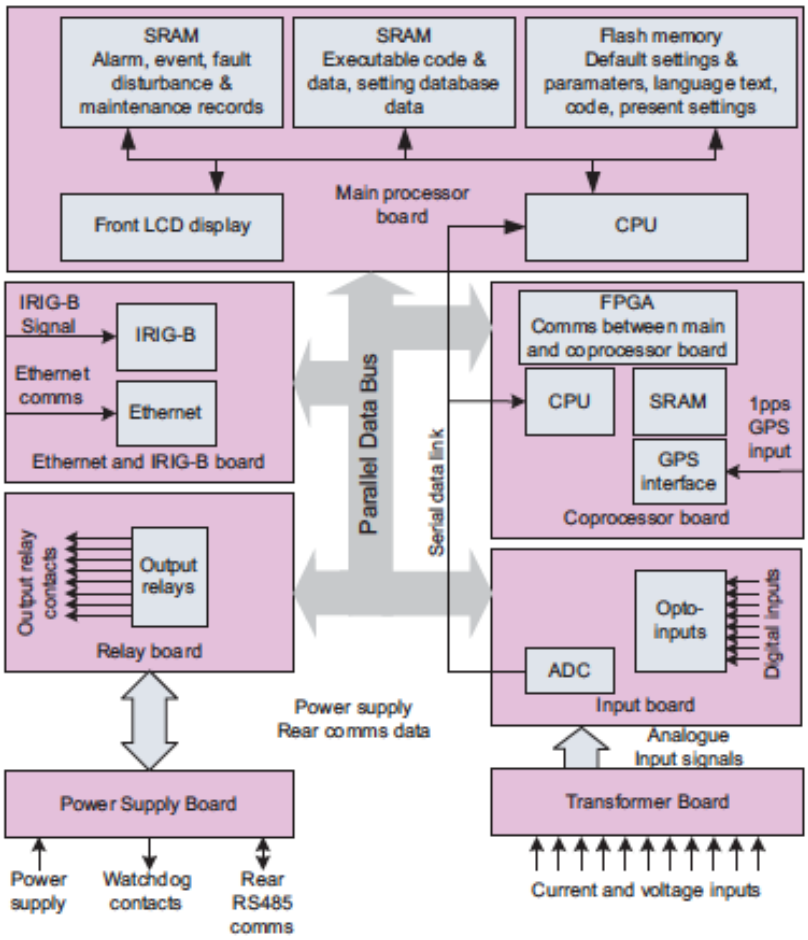

Figure 3.9: Typical architecture of numerical relay hardware [11]

With modern numerical relays, the matching and processing of the measured values is done numerically [26]. Signals are in the numerical relay converted from analogue to digital form using A/D converters. A modern numerical can sample each analogue input at between 24 to 80 samples per cycle [11]. It is important that measured values from multiple CT's are always sampled synchronously, as this is the only way to allow for a direct comparison. The value acquisition and processing scheme of a numerical relay is shown in figure 3.10.

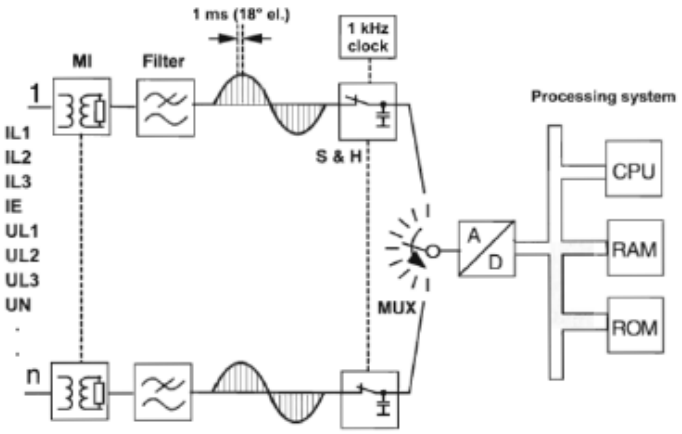

Figure 3.10: Measured value acquisition and processing [26]

3.6 Possible solution methods

3.6.1 Implementing a fixed time-delay for the Distance protection

Upstream distance relays and distance protection function in primary relay will work as back-up protection in the event were the primary protection relay does not clear the fault within a given time. One possibility to prevent the back-up distance protection from tripping if there is a fault during a zero-miss situation, is to calculate the duration of zero-miss and set the time delay accordingly. This solution would be fixed time delay regardless of any present of zero-miss and will therefore allow fault current to flow for a needless amount of time, when the switching angle is not exactly zero degrees. For a majority of the faults, the fault would be present longer that necessary and hence this is not the most optimal solution.

3.6.2 Make the sequential switching "smarter"

If a component on the breakers themselves can detect zero-miss and prevent the CB from an attempted opening, there will be no potential damage to the CB. In order to make the switching "smarter" there needs to be created some hardware connected to the CB. Alternatively it must be investigated if the switching controller used to control the switching instant of the phases can be used.

3.6.3 Implement a logic in the relay that prevent a trip signal during zero-miss

If the relay can detect that there will be a DC-current running trough the CB, it can be programmed not to trip the CB. The relays are already connected to a CT's so all the information required to determine zero-miss is already available as long as the CT is capable of reproducing both the AC and DC component. Both the Siemens and the ABB relays installed at at Indkildedalen are relays that are programmable. Both relays must send a trip signal in order for the CB to open its contacts and it is therefore sufficient to program one of the relays to block its trip signal in order to prevent the CB from operating.

3.7 Conclusion of problem analysis

The first solution method will not be an ideal solution and is discarded. The two relays already have the logic capability and access to the measurements from the CT's and VT's needed in order to detect zero-miss and prevent a trip from being sent. The solution to make a logic in the relays that prevent a trip onto a DC current is seen at the best solution strategy and will be the solution approach in this thesis.

3.8 Problem Statement

This M.Sc thesis seeks to develop a protection scheme that takes the zero-missing phenomenon into account for the operation of both the primary and the secondary protection.

The solution to the problem that has been investigated in this chapter can be divided in to the following partial objectives:

Objective 1: Simulate dynamic fault using PSCAD/EMTDC

Objective 2: Develop a logic so that the relay detects zero-miss and avoid trip signal

Objective 3: Propose a protection scheme and if time permits, validate it using a relay and OMICRON transient replay in laboratory

3.8.1 Key assumption and limitations

- It is assumed that information regarding switching instant is available in the relay

3.8.2 Prior work in the field

The effect on zero-missing phenomena has been thoroughly investigated in [5] [4] [2]. A protection scheme for a primary protection using sequential switching and additional circuit breakers on the shunt reactor to counter zero-missing was proposed in [6]. Energinet has also analyzed the cable connection under study in this report in [18], but the protection scheme was not addressed.

3.8.3 Solutions approach

The problem analysis gives a theoretical overview of the subject. A dynamic model of the cable+shunt reactor will be developed in PSCAD. The current output from these fault investigations will be extracted and used to design the relay logic that detects zero miss. The SIPROTEC relay will be chosen as the relay were a logic to detect zero miss will be implemented. The logic will be programed with CFC trough the software Digsi4. CFC blocks provides the means to implement user defined functions in Digsi4 which is the software that is used to program SIPROTEC relays. If time permits the solution will be tested at the laboratory.

3.8.4 Expected results

This thesis will design a protection scheme that can handle zero miss for both primary and secondary protection relay.

3.9 Summary

The chapter started with explaining operation of the circuit breaker and why a zero miss could cause a problem for the CB.The issue of zero-missing has ben thoroughly investigated along with possible countermeasures. After knowledge about the issue was established a final problem statement was formulated. The next chapter will present the modeling of the system.

Chapter 4

Modeling

This chapter will present how the modeling of the network under study has been conducted and the arguments presented to justify the choice of models. The software used to model the system in this thesis is PSCAD

4.1 Voltage source

The system under study is a 50 Hz network with a voltage level of 400 kV. The purpose of this model is to simulate faults and the short circuit current at the substation FER is obtained from Energinet.dk to be 14.906 kA. The source impedance is calculated using equation 4.1

$$Z_s = \frac{V_s}{\sqrt{3} * I_f} == 0.9188 + j15.466 \tag{4.1}$$

The voltage source is modeled in PSCAD as a voltage source behind the fault impedance as shown in figure 4.1.

4.2 Modeling methods for transmission lines

The cable at Indkildedalen must be properly modeled in order to simulate zero-miss and different fault scenarios. Depending on the required detail of the model, the transmission line can be modeled using different types of models like nominal π-model, Bergeron model or Frequency-dependent phase model among others.

4.2.1 Nominal π-model

The nominal π-model is based on the lumped R, L and C parameters for the actual transmission line, with coupling to ground considered. The distribution of the

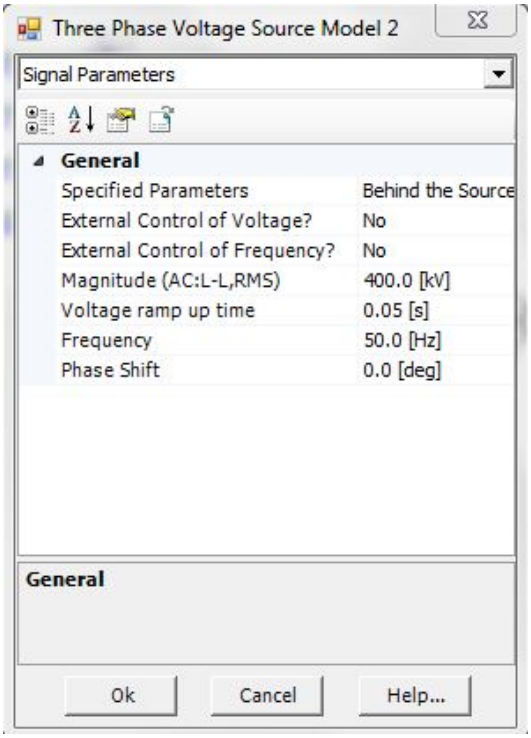

Figure 4.1: Voltage source configuration in PSCAD

parameters is not taken in to account as the lumped parameters are simply multiplied with the length of the line. Due to the lumped parameters of the inductance and the capacitance in the π-model, there is a possibility for a resonance at high frequencies that only is present in the model [31].

4.2.2 Exact π-model

This model includes the hyperbolic corrections with no approximations involved and is the best model for frequency scans and steady-state solutions [32]. The exact π-model is the most accurate model known and often used for frequency scan mathematical validation for frequency scan of other models [31]. The parameters Z and Y is calculated by equation 4.2 and 4.3 presented in [31]

$$Z = Z'l(\frac{sinh(Z'Y')^{\frac{1}{2}}l}{(Z'Y')^{\frac{1}{2}}} \tag{4.2}$$

$$Y = \frac{Y'l}{2}(\frac{tanh(Z'Y')^{\frac{1}{2}}l}{\frac{(Z'Y')^{\frac{1}{2}}l}{2}} \tag{4.3}$$

4.2.3 Constant-Parameter Distributed Line (Bergeron) model

The Bergeron model is a simple constant frequency method based on travelling wave theory. The inductances and capacitances of π-sections are represented in

a distributed manner [33]. The model incorporates travelling wave delays via a Norton equivalent circuit containing a current source and a constant resistance representing the characteristic impedance [33].

The Bergeron model is shown in figure 4.2:

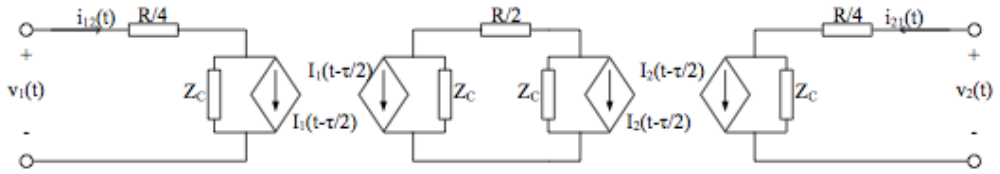

Figure 4.2: Bergeron model of a transmission line [31]

The lumped resistances are represented by dividing the line length into two sections, where each end has $\frac{1}{4}$-part of the resistance and the centre the remaining $\frac{1}{2}$-part [31].

4.2.4 Frequency-dependent phase-model

Frequency dependent models provides an accurate representation of the distributed nature of all line parameters and their frequency dependance [32]. The FD-model is based on travelling wave theory and has all RLC parameters distributed and without any lumped parameters [31].

There has been made much more publication regarding frequency dependent transmission line modeling than any other transmission line modeling techniques [31]. Advancements in frequency dependent transmission line models include the frequency dependent phase-models also known as Universal line model.

4.2.5 Method determination

The important aspects to model in this thesis is zero-miss and also faults in the transmission cable line. According to Table 5.2 in [5], lumped parameters would be sufficient for zero-miss while fault studies requires Bergeron model. However, the size of the model is limited and therefore the increase of simulation time using the more accurate frequency dependent phase-model will not pose a problem an is therefore chosen.

4.3 Cable Modeling

As it was decided in the previous section, the cable will be modeled using the frequency-dependent phase model. The fault current is affected by the bonding details and therefore cross-bonding of the cable will be modeled.

Cable laying The cables are laid in flat formation, cross-bonded and has been modeled in PSCAD as shown if figure 4.3

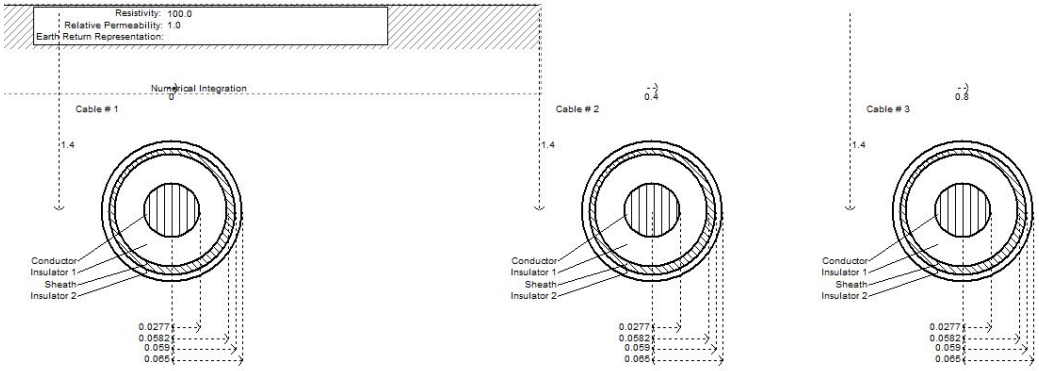

Figure 4.3: Cable configuration in PSCAD

Conductor In most modeling software, including PSCAD, it is only possible to model the conductor as a solid or a hollow conductor [31]. The cable to be installed at Indkildedalen is a segmental conductor and hence not a solid or hollow conductor. In order to compensate for the segmental conductor, the resistivity must be increased. The DC resistance is given in the cable data but for 20°C which means it first has to be adjusted to 90°C as shown in equation 4.4 [5]

$$\begin{aligned} R_{DC}(T) &= R_{20^\circ}(1+\alpha_T(T-20^\circ)) \\ \Rightarrow R_{DC}(90^\circ) &= 0.0149\Omega/km(1+4.03*10^-3(90-20)) = 0.0191\Omega/km \end{aligned} \tag{4.4}$$

Now the corrected resistivity can be calculated using equation 4.5 [31].

$$\rho' = R_{DC}(90^\circ)\frac{r_1^2\pi}{l} = 0.0191\Omega/km\frac{27.7mm^2\pi}{1.43km} = 3.22*10^-8\Omega/m \tag{4.5}$$

where:
ρ' is the corrected resistivity

Insulation and semi-conductive layers The first insulation layer consists of cross-linked polyethylene with a minimum thickness of 27 mm with an inner and an outer semi conductive layer of thickness 2 and 1.5 mm, respectively. The relative permittivity of insulation is normally between 2.3 and 2.5 [5].

The impact of the semi conductive layers are included by expanding the thickness of the insulation and increasing the relative permittivity [31]. The capacitance between the conductor and the screen can be calculated using equation 4.6 [31].

$$C = \epsilon\frac{2\pi l}{ln\frac{a}{b}} \tag{4.6}$$

Assuming the capacitance and length of the cable to be constant, the corrected permittivity can be calculated using 4.7 [31]

$$C = \epsilon' \frac{2\pi l}{ln\frac{r2}{r1}} = \epsilon \frac{2\pi l}{ln\frac{a}{b}} \Rightarrow \epsilon' = \epsilon \frac{ln\frac{r2}{r1}}{ln\frac{b}{a}} \tag{4.7}$$

where:
ϵ is the relative permittivity of the insulation
b is the outer and a the inner radius of the insulation
ϵ' is the corrected permittivity
r2 is the inner radius of the screen and r1 is the outer radius of the conductor

The corrected permittivity then becomes:

$$\epsilon' = 2.5 \frac{ln\frac{0.0582}{0.0277}}{ln\frac{0.0567}{0.0297}} = 2.87 \tag{4.8}$$

the outer screen The outer screen is made of a solid aluminum tape and therefore no correction of resistivity is required. The resistivity of the aluminum tape is $2.82 * 10^{-}8\ \Omega/\mathrm{m}$

Outer Insulation and extruded semiconductive layer The outer insulation consists of high density polyethylene with a minimum average thickness 6 mm.

PSCAD input parameter In PSCAD the cable is modeled with four main layers where the first insulation layer also included the two semi-conductive layers. The input parameter for the 4 layers in the cable as modeled in PSCAD is shown in table 4.1

The cable as it is modeled with minor sections and cross bonding in PSCAD is shown in figure 4.4

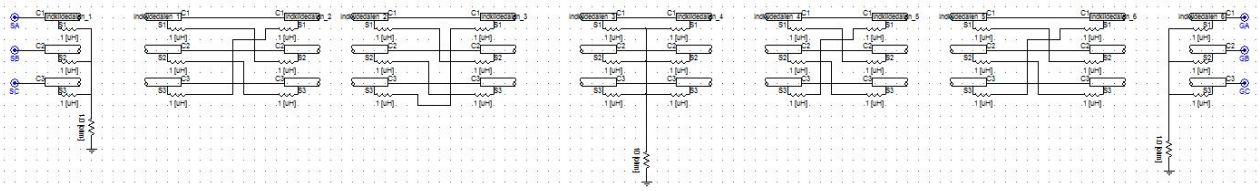

Figure 4.4: Overal cable configuration in PSCAD

Exact cable values for R, L and C Now that the cable is accurately modeled is is possible to get the exact values for R, L and C for the cable trough PSCAD. One cable section is chosen, the outer most conductor is eliminated and the cable is solved for constants. This gives the positive sequence resistance, reactance and susceptance for the cable section in per unit based on a 100 MVA base. The values must be multiplied with six since the cable consists of six identical cable sections.

Cable parameters		
Layer	**Parametres**	**Values**
conductor	resistivity	3.22*10^{-}8 Ω $/m$
	Outer radius	0.0227m
	Relative permabillity	1
Insulation layer 1	outer radius	0.0582m
	Relative permittivity	2.87 F/m
	Permabillity	1
Screen/Sheat	outer radius	0.059m
	Resistivity	2,8*10^{-}8 Ω $/m$
	Permabillity	1
Insulation layer 2	outer radius	0.065m
	Relative permittivity	2.5 F/m
	Permabillity	1

Table 4.1: PSCAD input parameters for the cable

Exact cable resistance is calculated using formula 4.10, inductance using 4.11 and capacitance using 4.13.

$$Z_{base} = \frac{V_{base}^2}{S_{base}} \tag{4.9}$$

$$Z_{ohm} = Z_{p.u} * Z_{base} \tag{4.10}$$

$$L = \frac{Xl}{\omega} \tag{4.11}$$

Susceptance is the inverse of the reactance and hence.

$$Xc_{p.u} = \frac{1}{B_{p.u}} \tag{4.12}$$

$$C = \frac{1}{\omega Xc} \tag{4.13}$$

The per unit values for resistance, reactance and susceptance is shown in table 4.2

The exact resistance, inductance and capacitance of the cable is calculated using the values from 4.2 and the formulas stated above. The values are multiplied by 6 to get the correct value for the entire cable and presented in 4.3

positive sequence values	
Unit	**Values**
Resistance	0.2155*10−3 pu
Reactance	0.2843*10−3 pu
Susceptance	0.0511 pu

Table 4.2: Measured values for one cable section in per unit

Exact cable values	
Unit	**Values**
Resistance	0.5701 Ω
Inductance	0.0024 H
Capacitance	1.5376 μF

Table 4.3: Values for the cable

4.4 Overhead line modeling

The overhead line model is also modeled using the frequency dependent model as the simulation time will not be significantly extended. The two sections of 1.81 km and 2.03 km has identical specifications and therefore they are modeled as one section with length 3.84km. The 6 conductors going from FER to SKH is modeled in PSCAD. The configuration of the 6 conductor delta tower and shown in figure 4.5

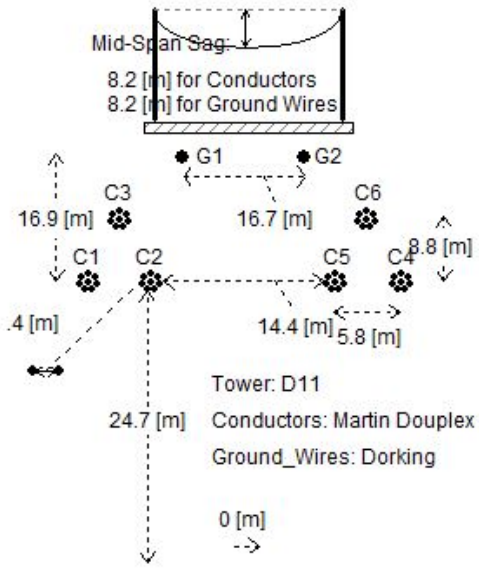

Figure 4.5: FER-SKH overhead line configuration in PSCAD

The phase wires are of Martin Duplex type and the ground wires are Dorking type. The data for the conductor and ground wire is shown in figure 4.6

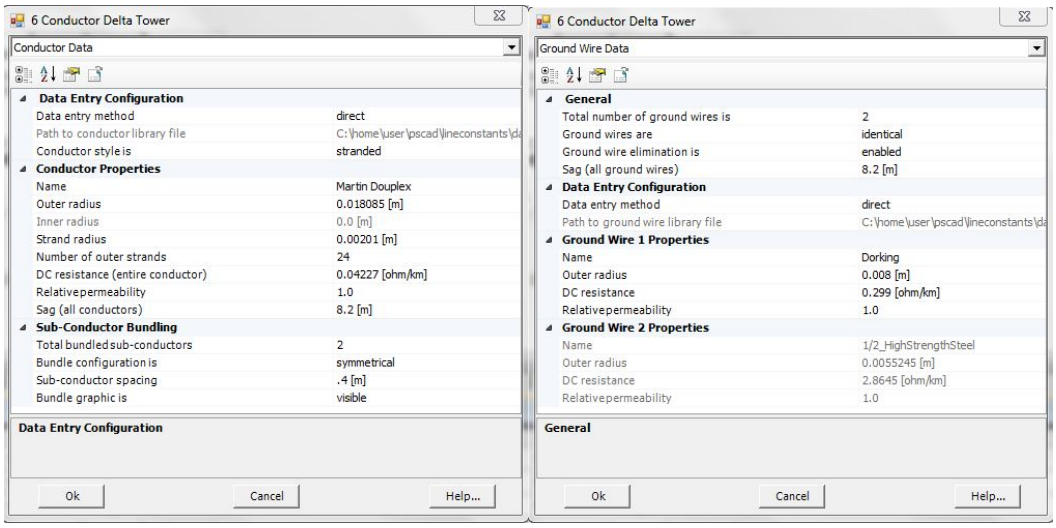

(a) Conductor data **(b)** Ground wire data

Figure 4.6: Feeder 4 in the map

4.5 Reactor modeling

The modeling of a shunt reactor is typically done with an inductor in series with a resistor and hence neglecting phenomenas like saturation, mutual inductance, magnetization losses, copper losses and additional losses like skin effect etc [5]. There are some mutual couplings between phases that has been measured in the test report [37] of the shunt reactor. The reactor was magnetized per phases in turn and the induced voltage on the other two phases was measured. The measurement was repeated for tap position 1, 15 and 29 which corresponds to 50, 71 and 110MVA, respectively. Mutual coupling can be modeled using a mutually coupled wire in PSCAD that requires the data for the coupling between A-B, B-C and A-C. The mutually coupled wire used in PSCAD is shown in figure 4.7 The mutual coupling for tap position 1, 15 and 29 is shown in table 4.4

In the mutually coupled wire it is assumed that the mutual coupling between phases are symmetrical, meaning that the mutual inductance between A-C=C-A, but as shown in table 4.4 this is not the case for the mutual inductance involving phase C. This is solved by simply taking the mean value of the mutual inductance between each phase. The new symmetrical mutual inductance involving phase C is shown in table 4.5

100% compensation rate is desirable and is calculated to L=5.4914 H for the exact value of capacitance of the cable from table 4.3. The reactive power to be compensated by the shunt reactor is calculated in 4.14

$$Q = \frac{V^2}{\omega L} = \frac{400kV^2}{2\pi * 50 * 5.4914} = 92.74MVAR \tag{4.14}$$

Mutual reactance		
Tap position	**Phase**	Ω
Tap 1	A-B	7.7
	B-A	7.6
	B-C	7.4
	C-B	7.7
	A-C	2.9
	C-A	2.1
Tap 15	A-B	4.9
	B-A	4.9
	B-C	4.8
	C-B	4.9
	A-C	1.9
	C-A	1.5
Tap 29	A-B	4.3
	B-A	4.3
	B-C	4.2
	C-B	3.5
	A-C	1.3
	C-A	1.0

Table 4.4: The mutual coupling between phases

Mutual reactance		
Tap position	**Phase**	Ω
Tap 1	A-C	2.5
	B-C	7.6
Tap 15	A-C	1.7
	B-C	4.9
Tap 29	A-C	1.2
	B-C	3.9

Table 4.5: Symmetrical mutual coupling between phases involving phase C

Mutual inductance	
Phase	**H**
A-B	-0.0146
B-C	-0.0140
A-C	-0.0046

Table 4.6: The mutual coupling between phases

Reactances are not given for 92.74 MVAR in the test report so interpolation has been used in order to find the tap position that compensates closest to 92.74 MVAR. Basic interpolation is shown in equation 4.15.

$$X1 = Xa + \frac{(Xb - Xa) * (Q - Qa)}{Qb - Qa} \tag{4.15}$$

where: as used here, X1 is the tap position that gives the desired reactive power compensation Q.

The result using interpolation shows us that tap position 22.81 gives the desired Q. Using the same interpolation procedure we find that tap 22 gives us 90.5 MVAR and 97.6% compensation. The inductance at tap position 22 becomes 5.6276 H.

After the new reactance's for tap 22 have been obtained also using interpolation, the inductance is calculating using equation 4.16

$$L = X_L/\omega \tag{4.16}$$

where: ω =$2\pi 50$

Using the values from table 4.5, equation 4.15 and 4.16 the mutual inductances is calculated and shown in table 4.6. These are the values that are are used in PSCAD for the reactor modeling.

The mutually coupled wire used to represent the shunt reactor in PSCAD is shown in figure 4.7. Saturation can be added by the means of three single phase transformers but is not included in this analysis as saturation will not affect the studies in this report.

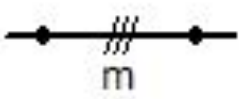

Figure 4.7: Mutually coupled wires in PSCAD

4.6 Complete model

The complete model that has been modeled in PSCAD is shown in figure 4.8. The model includes a voltage source, the overhead line from FER to SKH, circuit breakers, shunt reactor and the cables in Inkildedalen.

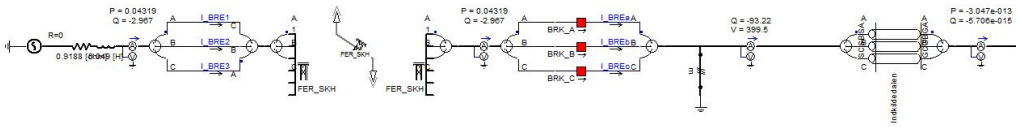

Figure 4.8: Complete model in PSCAD

4.7 Summary

The parameters of each component has been calculated in this chapter and modeled in PSCAD. The final model was presented at the end go the chapter and the simulations will be shown in chapter 5.

Chapter 5

Simulations

The three-phase simulation using PSCAD shows similar characteristics for energization of the cable at zero voltage, compared to the single phase, pi-model simulations presented in chapter 3. The switching of the phases takes place a voltage zero crossing for each phase and a current zero missing phenomenon is clearly present. Voltage at the switching instant and the current trough the CB is shown in figure 5.1.

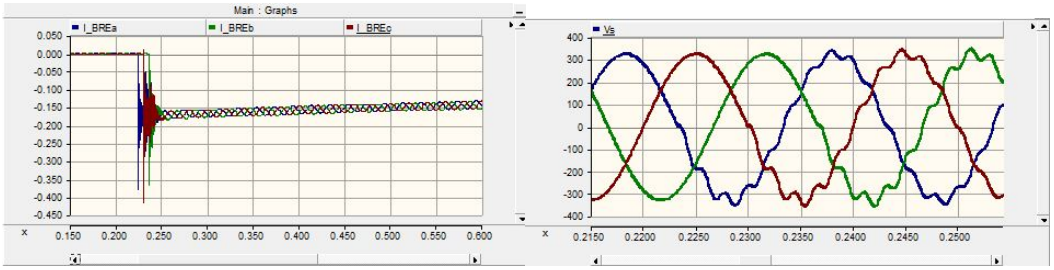

(a) Current at the CB **(b)** Voltage at the CB

Figure 5.1: Zero-missing shown for switching at zero voltage

5.1 Fault Analysis

A fault is now applied to the network in order to see the behavior of the waveforms in the presence of different faults. The different types of faults needs to be simulated in order to get a current output that can be used as input current for the relay. This input current can be used in order to test the tripping logic. The two fault scenarios that will be investigated are the phase to ground fault and two-phase to ground fault. Any three-phase to ground fault would not be relevant for this report as there will be zero-crossing present in all three phases and the relay can operate as usual.

5.1.1 Single-phase to ground fault

A single-phase to ground fault was imposed on one of the cable sections as shown in figure 5.2. It can be seen from figure 5.3 that the phases are energized at zero crossing, around 0.23s and that a single-phase to ground fault occurs after 0.4s. The two healthy phases does not have the fault current running trough them, and therefore the zero missing is still present in those phases. The voltage curves at the fault instant is shown in figure 5.4

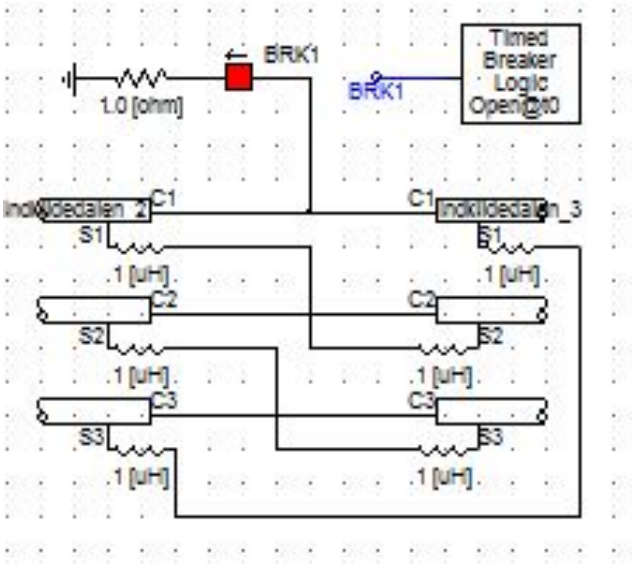

Figure 5.2: Single-phase to ground fault in cable

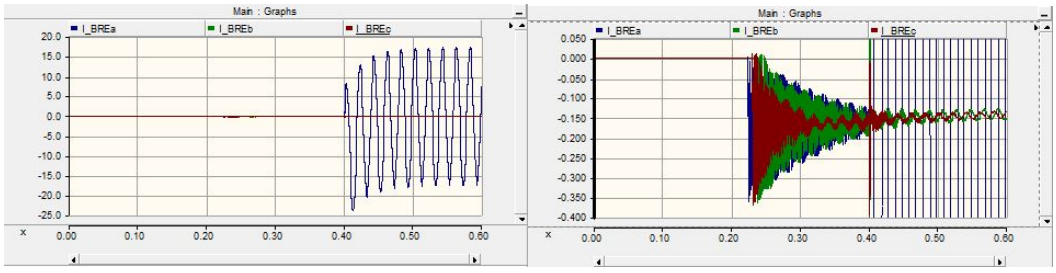

(a) Scaled after fault current **(b)** Scaled to healty phases

Figure 5.3: Single-phase to ground fault

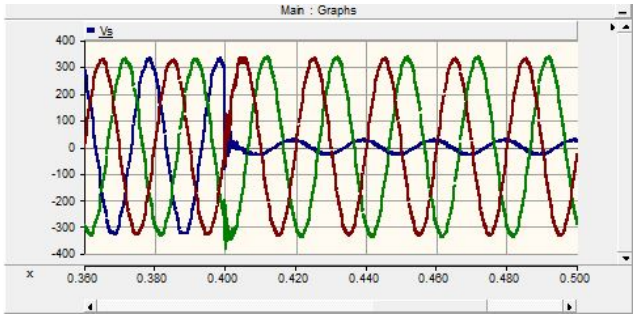

Figure 5.4: Voltage curve for single-phase to ground fault

5.1.2 Two-phase to ground fault

A two-phase to ground fault in the cable is imposed on one of the cable sections as shown in figure 5.5. The two-phase to ground fault in the cable would lead to a fault current running in two of the phases as shown in figure 5.6. It can be seen that there is zero missing only in the remaining healthy phase. The voltage curve at the fault instant is shown in figure 5.7

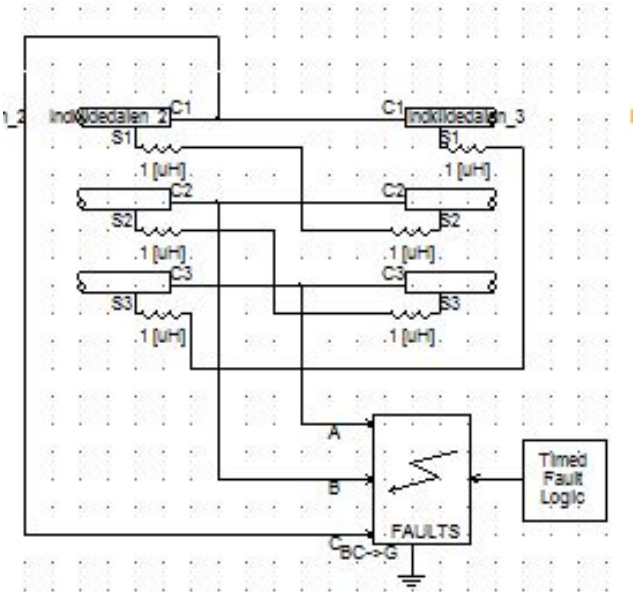

Figure 5.5: Two-phase to ground fault in cable

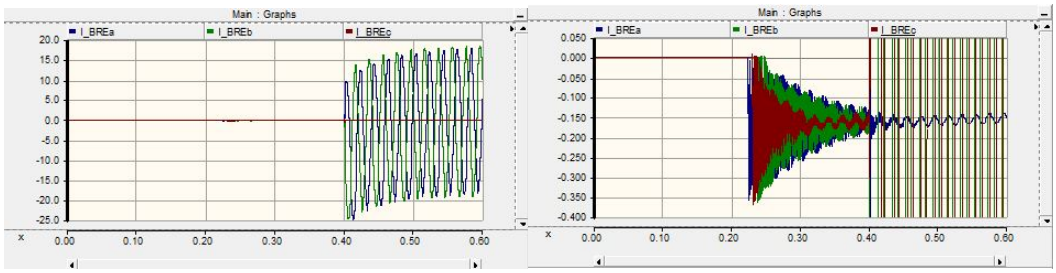

(a) Scaled after fault current **(b)** Scaled to healty phases

Figure 5.6: Two-phase to ground fault

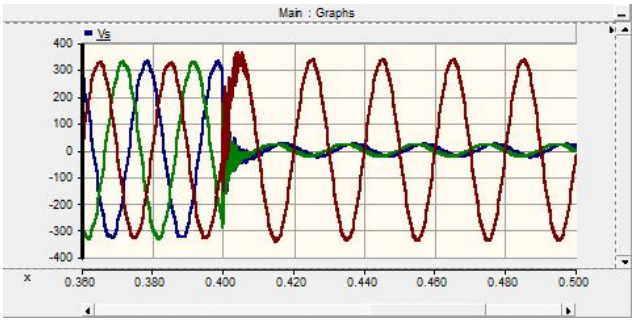

Figure 5.7: Voltage curve for two-phase to ground fault

Chapter 6

Problem solving

In this chapter the reader will be introduced to different possible solution strategies that will been further investigated. Different ways of enabling the relay to detect zero-miss will be shown along with challenges associated with the solution strategy. The purpose of this chapter is to propose several solution methods in order to create a broad specter of solution strategies that can be applied under different circumstances. Only two will be chosen for further investigation and implemented in chapter 7.

6.1 Determine zero-miss based on input current directly

The solutions in this section in based on the idea that the relay has all the information it requires in the input current and is able to determine when zero-crossing will occur.

6.1.1 Calculate zero-crossing

It is suggested two ways for the relay to mathematically calculate zero-crossing, one based on separating the AC from the DC component and the other one using the whole signal intact.

Separate AC and DC component of the current One method is just the same as used in section 3.3 to calculate the exact zero-crossing. The AC component must be separated from the DC component and zero crossing is found by setting the AC peak value + the DC component to zero. The current is filtered once it enters the relay and the dc component is removed from the ac signal. The filtered "pure" ac signal can then be subtracted from the original signal to get the DC component. Zero-crossing can then be found by setting the AC and DC signal equal to each other and solve for t.

Use total current Given the input current with its AC component and its DC offset. Zero crossing can be solved by solving the equation for the input current by setting the current to zero and solve with respect to time. Another possibility is if the relay has a block capable of comparing the input signal directly to zero. The relay can then calculate zero-crossing directly and block any trip signal until zero-crossing is present. This requires the relay to either be able to compare a signal directly to zero or be able to solve equations with the respect to time.

6.1.2 External device that can send a blocking signal to the relay

An external device between the relay and the CT can be installed as shown in figure 6.1

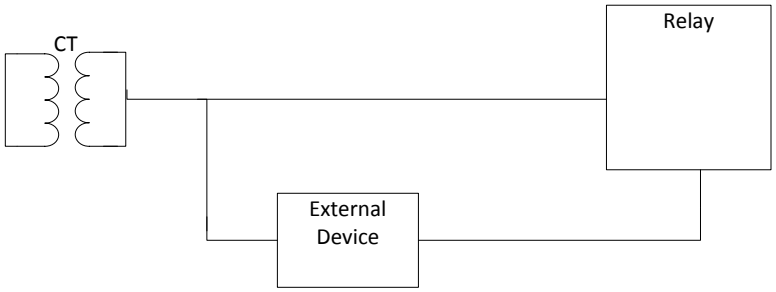

Figure 6.1: External device used to detect zero-miss

Fast Fourier Transform If the current from the CT goes to a box with FFT (fast fourier transform), all the frequencies of the signal and their values would be detected. The decaying DC component can be seen as a low frequency AC component detectable by the FFT. If the DC magnitude is more that half of the AC magnitude this leads to the conclusion that there is current zero-missing. Based on the information of the values for the AC and DC signal a blocking signal can be sent to the relay. A fast fourier transform was conducted on the signal using simulink and presented in figure 6.2. It can be seen that the magnitude of the DC component is found as a percentage of the fundamental 50 Hz AC signal. By doing a FFT analysis for each cycle it is possible to get the DC value as a decaying component separated from the AC component.

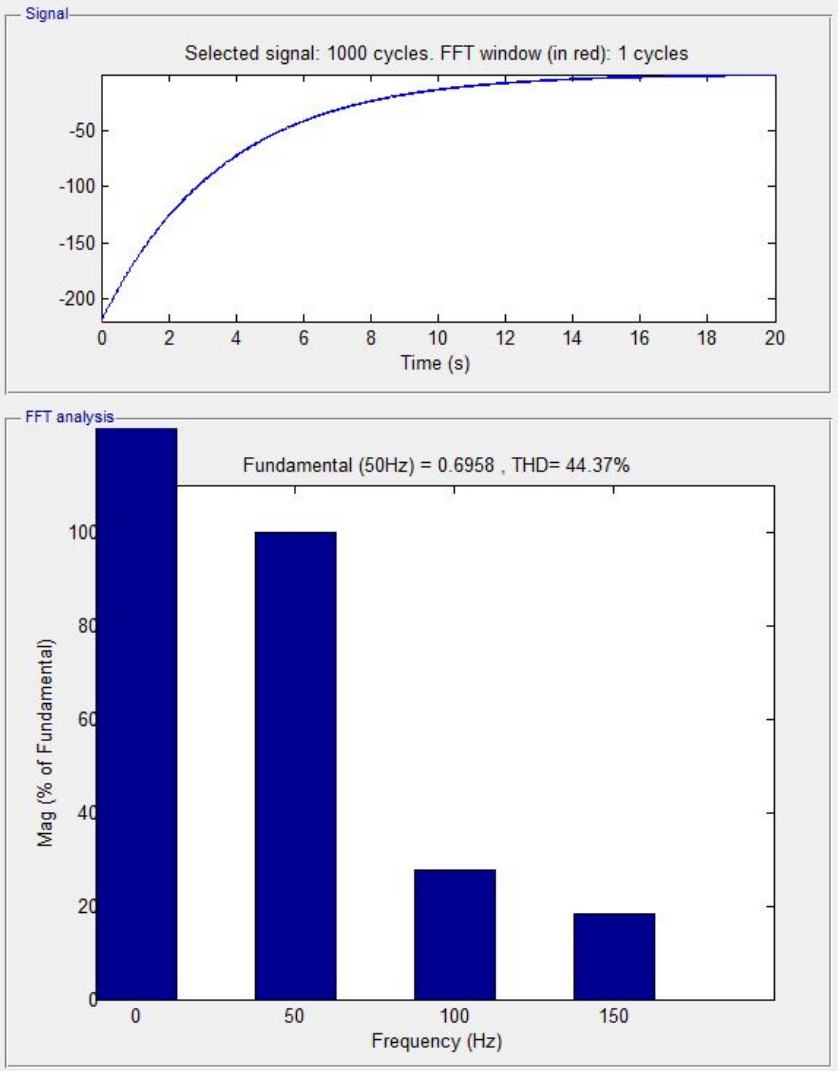

Figure 6.2: A FFT analysis of the input current

External filter A external high-pass filter can be put in the box in order to filter the signal so that only the 50 Hz AC component is present. Figure 6.3 shows the current before and after the filter

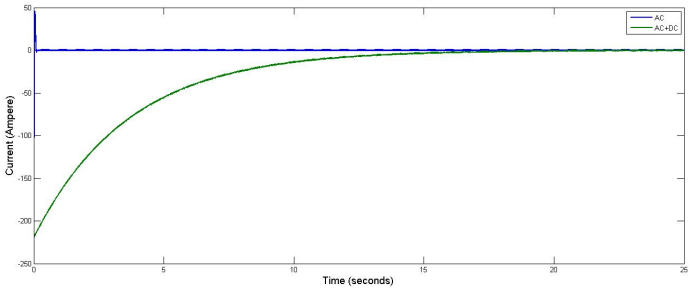

Figure 6.3: The current shown before and after the filter

It can be seen that the dc-offset has been removed from the current and that there is only the AC signal left. The next step is to subtract this AC component from the original signal to get the DC component. The DC component of the signal os shown in figure 6.4.

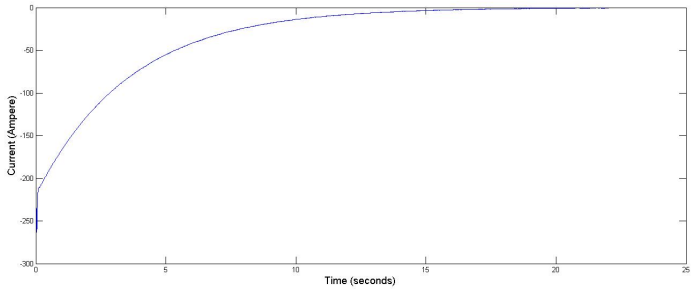

Figure 6.4: The extracted DC-component of the current

By the use of the external device, the AC and DC components can be sent too the relay and be made available as inputs in CFC, used as input in an relational operator or used to create a blocking command sent to the binary input of the relay. The relational operator would have output 0 and 1 for AC≠DC and AC=DC, respectively.

6.1.2.1 DC-component detection

All suggestions presented above assumes that zero-missing is present in the input of the relay when it is present in the main circuit. This depends in the ability of the measuring device used to replicate the main current.

The by far most used analog input element in protection relays is the current transformer (CT). In order for the relay to be able to see the zero-missing, the CT has to be able to reproduce the dc offset present in the primary circuit to the secondary circuit. An ideal CT would replicate the primary current to the secondary current by a factor depending of turns ratio. For an actual CT it becomes a bit more complicated and we need to look at the transient response of the CT in order to se if the DC component will successfully replicated on the secondary side of the CT.

Transient response of current transformers No conventional CT has the ability to continuously reproduce a DC component present in the primary current. However, different types of CT's has more or less capability to reproduce a decaying DC component over a limited interval of time [39]. There are several different classes and standards of current transformers but all can essentially be divided into three types of conventional CT's depending on the iron core and the presence of air gap [40] [13]:

- High Remanence (HR) type is a closed core CT with no deliberate limitations put on the remanence flux. This type if CT has a core without any air gap

and a remanent flux may remain for almost an infinite time. The remanent flux can be up to 70-80 % of the saturation flux in a HR type CT. Typical types of high remanence type CT is P, PX, TPS and TPX according to IEC 60044-1 or 61869-2.

- Low Remanence (LR) type is a CT with a small "anti-remanence" air gap to reduce the remanent flux so that the level does not exceed 10%. A typical low remanence CT is a PR or TPY according to IEC.
- Non-Remanence (NR) type is a CT with a relative big air gap in order to reduce the remanent flux to a practically zero level. A TPZ is non-remanence type of CT

The high remanence (HR) type CT's transform the DC and AC component within the defined range with high accuracy [13]. A non-remanence CT severely damps the DC component in the transformation, giving the CT poor abilities to reproduce the transient DC component [39]. This means that the indicated transformation accuracy in a NR-type CT only applies to the AC component as the DC component is heavily attenuated [13]. A Low remanence (LR) type is somewhere in between a HR and a NR type CT when it comes to its ability to reproduce the DC component. According to [39] it will reproduce a DC component but contrary to the HR, the error from the primary circuit to the secondary using a LR type is not negligible.

To explain the effect of the air gap on the CT's ability accurately replicate the primary current we first need to study the equivalent circuit of a current transformer as shown in figure 6.5

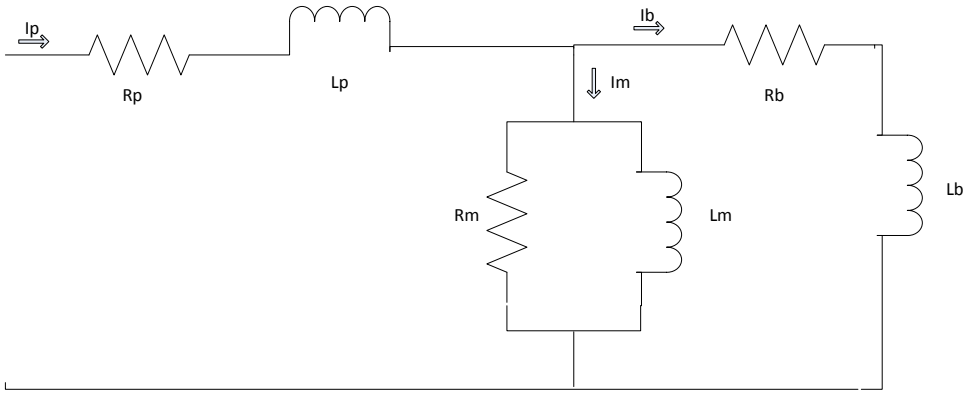

Figure 6.5: Equivalent circuit of a CT

From the equivalent circuit, the voltage and current equations are [38]:

$$L_m * \frac{di_m}{dt} = R_b * i_b + L_b * \frac{di_b}{dt} \tag{6.1}$$

$$i_m = i_p - i_b \tag{6.2}$$

substituting equation 6.2 in to 6.1 and solving for the derivative of i_b yields [38]

$$\frac{di_b}{dt} = \frac{L_b}{L_b + L_m} * \frac{di_p}{dt} - \frac{R_b}{L_b + L_m} * i_b \tag{6.3}$$

Equation 6.3 is the current that the relay will see as its input current for a current i_p in the primary circuit.

Now back to the ability to replicate the current running in the primary circuit. The introduction of an air gap in the core would reduce the magnetization inductance (L_m) which leads to i higher magnetization current. The output secondary current that the relay sees is $i_b = i_p - i_m$ and hence the introduction of an air gap in the core leads to higher attenuation of the secondary current.

The most commonly used current transformer by energinet.dk is the Siemens 5PR30 which is a low remanence type CT. Measurements done by energinet.dk shows that zero-missing is present and hence the CT is capable of replicating a decaying DC component. However, this does not give any information regarding the error between the replicated current in the secondary windings compared to the actual current running trough the circuit breaker. A simulation in PSCAD shows that the DC-component is being damped faster on the secondary side of the CT compared to the current in the primary circuit. This is shown in figure 6.6.

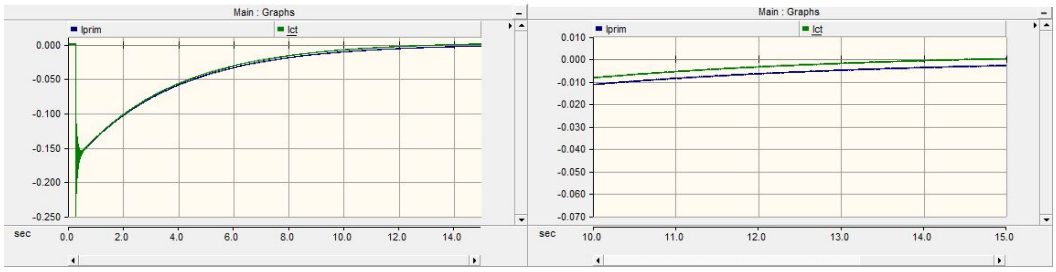

(a) 1-15s scaled window **(b)** 10-15s scaled window

Figure 6.6: Zero-missing shown for primary and secondary side of the CT

It can be seen that the CT secondary current cross zero after 9s while it is shown in section 3.3 that the current in the primary circuit cross zero 4 seconds later. Due to this error it is of interest to look for a solution independent of the CT accuracy.

6.2 Based on switching instant and time constant

This method is not depending on the input current and is therefore not affected by any error in the CT current transformation. The point on wave switching instant for the energization of the cable is information that will be present in the relay. One possibility is therefore to implement a logic that uses equation 3.21 presented in section 3.3, which calculates the duration of zero-miss based on the switching instant and the value of the inductance and resistance of the shunt reactor. The

equation is repeated in 6.4 [5].

$$t = -\frac{Ls}{Rs} * ln|\frac{(x-1)}{(xcos\theta)}| \tag{6.4}$$

A simple block implementation of equation 6.4 made in simulink and shown in 6.7

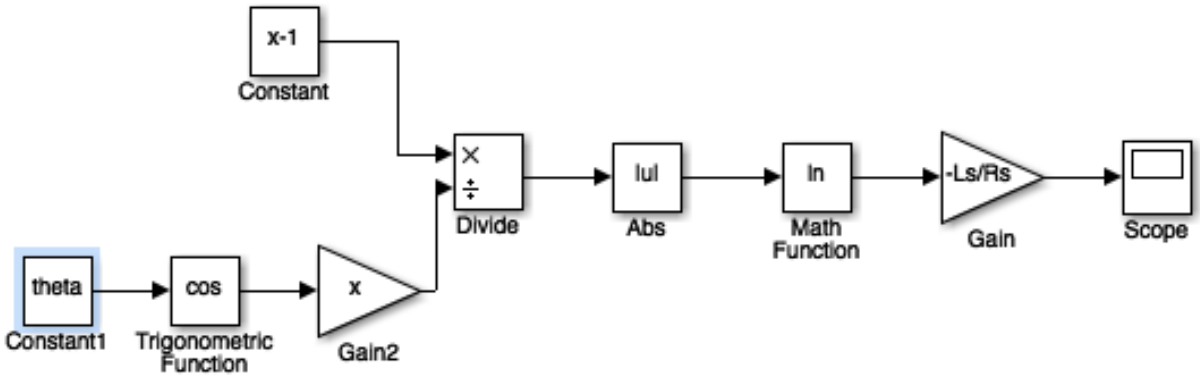

Figure 6.7: Block diagram for calculating duration of zero-miss

The formula is based on an ideal voltage source and therefore the values of the inductance and resistance will be affected by the system when this equation is used in a real network. The $\frac{X}{R}$ ratio of the system are smaller than for only the shunt reactor. Using equation 6.4 would therefore indicate a longer time without zero-crossing compared to the real current. This can symbolize a worst case scenario or a safety margin. The only input needed to implement this equation in a logic is the point on wave switching instant θ that can be detected by a switching controller, VT etc.

As mentioned in section 3.3, this formula will not be valid for 100% compensation as you will be taking ln to zero. The compensation ratio is decided by the tap settings of the shunt reactor it was shown in section 4.5 that 100% compensation is not possible but tap 22 gives 97.6% compensation. This level of compensation is calculated using equation 6.4 to give zero-crossing after 13.033s while the exact calculation using laplace as demonstrated in section 3.3 gives a zero-crossing after 12.999s. The prolonged duration of zero-miss calculated by 6.4 can be seen as a 34 ms safety margin. As mentioned previously, the biggest error would come from the difference between the actual time constant of the system and the time constant used for the shunt reactor.

6.3 Summary

Different solution strategies based on available information was investigated in this chapter. The first approach assumes that the input current into the relay is an

accurate replication of the actual current in the system. This was shown in subsection 6.1.2.1 to not necessarily be correct. The other approach was to use a formula for calculating zero crossing based on the $\frac{L}{R}$ ratio, switching instant for the cable energization and the compensation ratio of the shunt reactor. Any error of significance related to this approach will be the error caused by using $\frac{L}{R}$ ratio of only the shunt reactor.

Chapter 7

Implementation in Digsi

The software used for parameterization and setting of SIPROTEC relays is Digsi 4. The version used in this thesis is Digsi V4.89 which was released in 2014. Two solution strategies are chosen to be implemented and tested in the relay, one depending on a accurately replicated current and one depending on switching instant and compensation ratio.

7.1 Accurate current input

The first implementation assumes that the input current into the relay contains both the AC signal and the correctly replicated DC signal. When that is the case it is possible to use a comparison block which is capable of comparing two inputs and give an output when they are equal. This block is used to compare the current on each phase to zero. This block is then connected to an "and" block along with any trip signal. Both the requirements needs to be fulfilled before a trip signal is sent to the CB. The implementation is shown in figure 7.1

The same comparison block can also be used for the methods where the AC and DC signals are separated as mentioned in chapter 6. To quickly summarize, current zero crossing is found by setting the AC and DC signal equal to each other. As proven in chapter 6, there are some errors associated with the CT transformation that favors an approach independent of the DC component of the input current.

7.2 Implementation of zero-crossing formula

The other strategy chosen to implement is depending on the switching instant when the cable was energized along with the compensation ratio and the $\frac{L}{R}$ ratio. The formula for calculating the approximate duration of zero-miss will be implemented into Digsi 4 in this section. The formula is repeated again for this chapter in

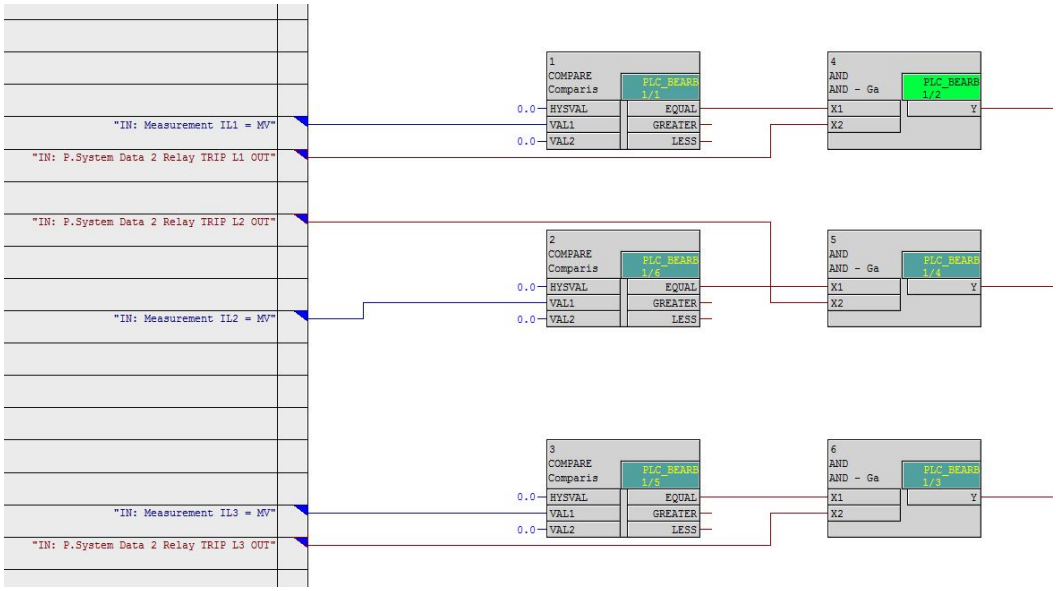

Figure 7.1: A simple CFC implementation to ensure "trip" only when zero crossing is present

equation 7.1 [5]

$$t = -\frac{Ls}{Rs} * ln|\frac{(x-1)}{(xcos\theta)}| \tag{7.1}$$

In Digsi 4 there is not any arithmetic blocks representing a logarithmic function, nor is there any blocks for cosine. The Arithmetic function blocks available in Digsi 4 are:

- ABSVALUE
- ADD
- DIV
- MUL
- SQUARE_ROOT
- SUB

It is therefore necessary to expand the logarithmic function using Taylor series and also approximate the cosine function. This is done in the following subsections

7.2.1 Expansion of logarithmic function

The logarithmic function is approximated using Taylor series and the point which the formula is approximated about is important. It is assumed that the rate of compensation will be 97.6% (tap 22) and that the switching will be made around 0 crossing. The point of which the Taylor series will be based around is shown in eq 7.2

$$point = |\frac{(x-1)}{(xcos\theta)}| = |\frac{(0.976-1)}{(0.95cos(0))}| = 0.0246 \tag{7.2}$$

The point 0.025 is chosen for the basis of the Taylor series and hence a_0 in the following equation. The Taylor expansion around the point a for the natural logarithmic function is shown in equation 7.3 [42]

$$ln(a) = ln(a_0) + \frac{1}{a_0} * (a - a_0) - \frac{1}{a_0^2} * \frac{(a-a_0)^2}{2} + ... \tag{7.3}$$

where ln(a_0)=ln(0.025)=-3.6889

7.2.2 Approximation of cosine

The next challenge is to approximate the cosine function. A indian mathematician by the name of Bhaskara presented a very accurate algebraic formula for approximating the trigonometric sine function sine function as early as the seventh century. His formula is shown in equation 7.4 [41].

$$sin(\theta) = \frac{4\theta(180-\theta)}{40500 - \theta(180-\theta)} \tag{7.4}$$

Related to cosine this equation shifted with 90 degrees as shown in equation 7.5. 90 degrees was stated instead of $\frac{\pi}{2}$ intentionally due to the fact that the angle must be stated in degrees for this formula to be valid.

$$cos(\theta) = \frac{4(\theta+90)(180-(\theta+90))}{40500 - (\theta+90)(180-(\theta+90))} = \frac{4(8100-\theta^2)}{32400+\theta^2} \tag{7.5}$$

The formula is applicable for θ in the range from -90 degrees to 90 degrees. The accuracy of Bhaskara's approximation compared to the actual cosine function is shown in table 7.1

Ratings			
θ	**cos(θ) by Bhaskara rule**	**Actual value of cos(θ)**	**error**
0	0	0	0
30	0.8649	0.8660	0.0017
45	0.7059	0.7071	0.0013
60	0.5	0.5	0
90	0	0	0

Table 7.1: Comparison on Bhaskara's approximation and actual cosine value

Bhaskara's approximation is implemented as chart 1 in Digsi 4 and shown in figure 7.2

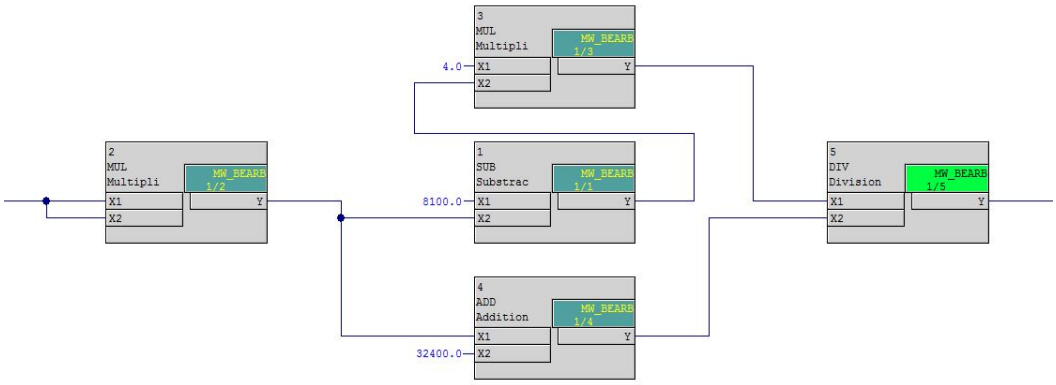

Figure 7.2: CFC Chart 1: Bhaskara approximation of cosine

7.2.3 Approximation of zero-crossing formula

The expression to be taken the natural logarithm to is the expression shown in 7.6

$$a = |\frac{(x-1)}{(xcos\theta)}| = |\frac{(x-1)}{x(\frac{4(8100-\theta^2)}{32400+\theta^2})}| \tag{7.6}$$

This is implemented in Digsi 4 by adding chart 2 as shown in figure 7.3

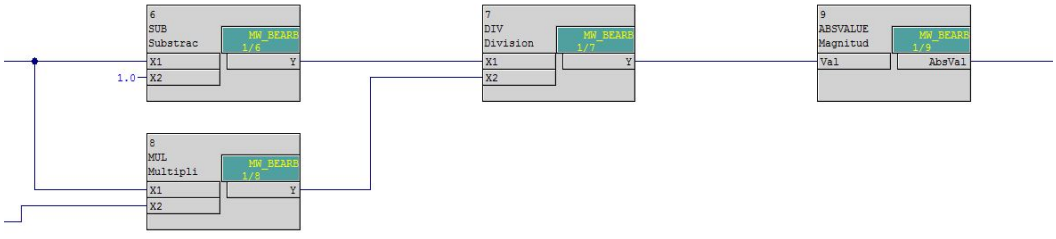

Figure 7.3: CFC Chart 2: x-function in ln(x)

Equation 7.3 and equation 7.6 must be combined in order to approximate equation 7.1. The final equation then becomes 7.7

$$t = -3.6889 + \frac{1}{0.025} * (|\frac{(x-1)}{x(\frac{4(8100-\theta^2)}{32400+\theta^2})}| - 0.025) - \frac{1}{0.025^2} * \frac{((|\frac{(x-1)}{(xcos\theta)}| = |\frac{(x-1)}{x(\frac{4(8100-\theta^2)}{32400+\theta^2})}|) - 0.025)^2}{2} + ... \tag{7.7}$$

where x is the compensation ratio
θ is the voltage "point on wave" at the instant of energization

7.2.4 validation of the approximation

Equation 7.7 is validated against equation 7.1 with the given parameters

- L=5.6278
- R=1.6
- θ=0
- x=0.976

The calculation using 7.1 yields the result 13.0328 s and the approximation made by 7.7 yields zero-crossing after 13.0334 s. A difference of 55.6 ms is regarded as very satisfactory as the phenomena last several seconds.

The third chart implemented in Digsi 4 comprises the final formula 7.7 and is shown in figure 7.4

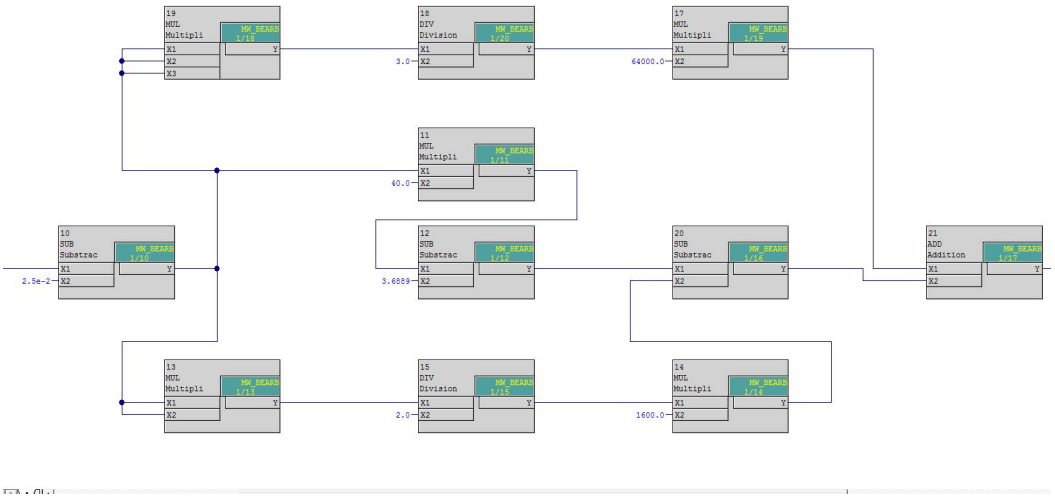

Figure 7.4: CFC Chart 3: Implementation of 3'rd degree taylor series of logarithmic function

It can be seen from chart 1 in figure 7.2 that the input θ which, is the point on wave switching instant, is set manually. In a real application the switching instant needs to be measured and the information made available for the relay logic. At the moment of switching, there are oscillations on the voltage curve. The

voltage waveforms are available to the relay trough the voltage transformers but the measuring functions in the relay are not quick enough to se the oscillations on the sine wave at the switching instants. Only the protective functions of the relay are capable of such rapid response.

It is the switching controller of the CB that insures that the breakers close at the desired point on wave. It is therefore assumed that the switching controlled has the information of the voltage waveform and when the switching were done. This information can then be put into the relay trough one of its binary inputs.

7.3 Summary

Two solution strategies were implemented in Digsi 4 in this chapter. The first and simplest implementation is based in the assumption of accurate input current and the second implementation assumes that the switching instant is available. Due to limitations in the Digsi 4 software, the formula for calculating zero crossing had to be approximated using taylor series and Bhaskara's sine approximation. The implementation was successful and the approximation was proven to be accurate.

Chapter 8

Results

Two solutions to avoid tripping a DC current in the event of zero-missing phenomenon were implemented into Digsi in chapter 7. The relay installed at Indkildedalen is a 7SD522 relay but unfortunately this relay is not available in the lab. However, a 7SA610 distance relay is available in the lab and used to test the implemented logic. The specific version of the relay used is 7SA6102-5AB02-0CA6/EE. The masking address 0110 Trip mode with the possibility of choosing 1 or 3 pole tripping is only applicable for devices capable of 1-pole tripping. It is a prerequisite that the device is provided with an internal automatic reclosure function or that an external automatic reclosure is used [43]. The relay available at the laboratory does not include this feature but the 7SD522 does.

It is however possible to create a 1 pole trip signal using CFC and route that signal to one of the other binary outputs. It is also possible to test the implementation using 3 pole tripping. The only alteration using 3 pole tripping is that the tripping of all three phases will be delayed until zero-crossing is present in order for the implementation to be successful.

The current depending solution strategy implemented in section 7.1 is tested by creating 1 pole tripping and the solution strategy to calculate time to zero crossing is tested using the 3 pole trip. Both implementations have been tested with the single-phase to ground fault from subsection 5.1.1 were the fault was applied after 0.4 s.

8.1 Test setup

The output current from generated in PSCAD in chapter 5 is used as the input current when testing the implementation. The output from PSCAD is stored in a comrade file and imported into the omicron transient replay. The Omicron CMC 356 device then outputs the currents into the 7SA610 relay. A picture of the test setup is shown in appendix A.

8.2 Testing of accurate current input implementation

No further implementations are required beyond the implementation explained in section 7.1. The oscillographic fault record for this implementation is shown in figure 8.1

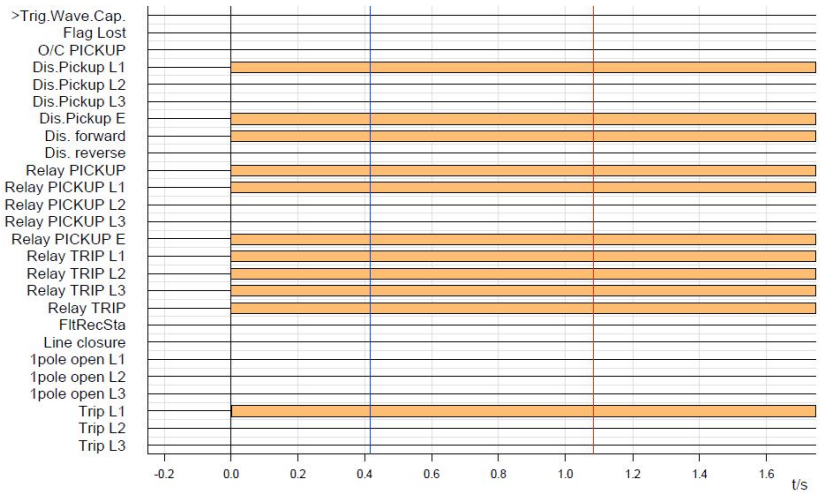

Figure 8.1: L1E fault with the accurate current input implementation

It can be seen from figure 8.1 that a fault in phase 1 and ground is detected. The relay sends a trip signal in all three phases since 1 pole tripping is not available. The logic uses the trip signal for each phase as input in the "AND" block. Only phase 1 with zero crossing has fulfilled the criteria set by the comparison block and is hence tripped.

8.3 Testing of zero-crossing formula implementation

The implementation of the time to zero-crossing formula with a 3 pole trip is shown in figure 8.2. The time to zero-crossing in seconds from chart 3 is used as input in Chart 4. The timer requires the input in ms so the signal must be multiplied by 1000 before it is used as input in the timer. The timer starts counting from zero and sends an output as soon at the timer exceeds the time to zero-crossing. The trip signal will be sent to the CB if a trip signal is present and the condition $t > t_{zero-cross}$ has been met. The oscillographic fault record is shown in figure 8.3.

Figure 8.3 shows that the relay pickup a fault in phase 1 (L1) and earth (E) and sends a trip signal to all three phases. It is not possible to suppress this trip signal from 00511 which goes to binary output 2 (BO2). It is however possible to connect the CB to another binary output linked to the trip signal from the implemented logic. This new trip signal is called New 3ph trip and as shown in figure 8.3 there is no trip signal from New 3ph trip due to the fact that $t < t_{zero-cross}$.

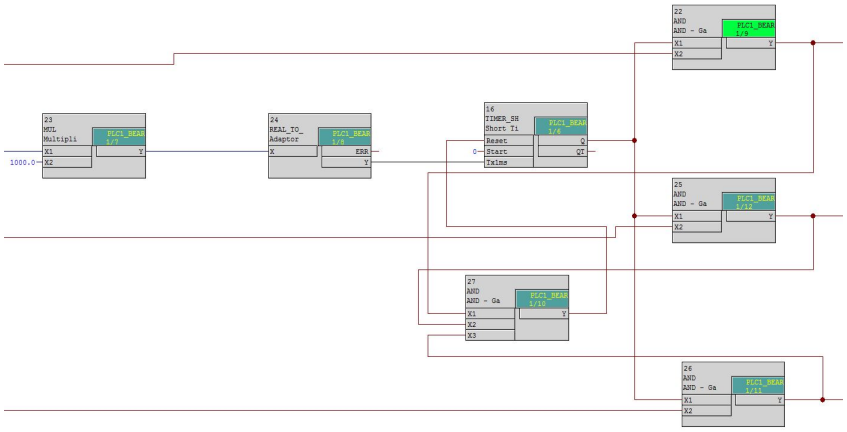

Figure 8.2: CFC Chart 4: Implementation of zero cross formula into trip circuit

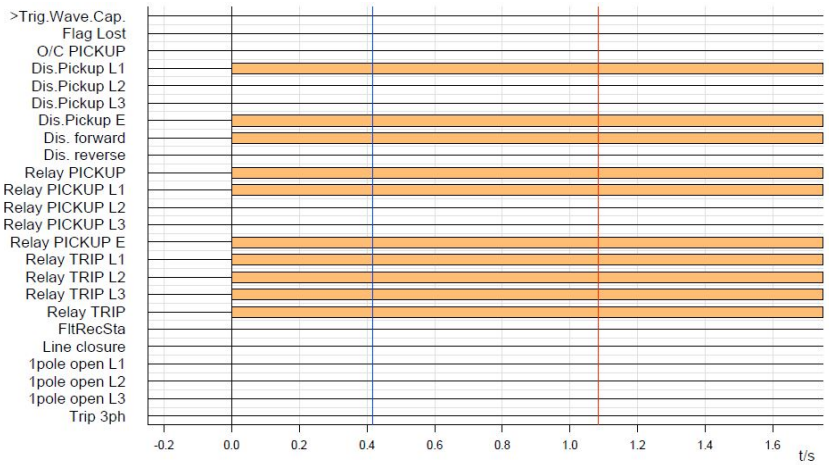

Figure 8.3: L1E fault with time equation implementation

8.4 Summary

The relay used in lab does not support 1 pole tripping but this can be done manually using CFC and signal routing. Both implementations from chapter 7 was tested against an unsymmetrical fault. Test results show that by using one of the implementations, the relay will not trip the healthy phases during an unsymmetrical fault if there is zero miss present. It must be added that further testing is required before a conclusion regarding the final success of these implementations can be made.

Chapter 9

Conclusion and future work

The objective for this project was to detect zero miss and control the circuit breaker in order not to open its contacts when zero miss is present. Zero missing phenomenon have been thoroughly investigated along with its consequences and countermeasures. It was concluded that the CB on the healthy phases would not be able to open its contacts if tripped due to a fault in the time period were zero missing is present.

Different solution strategies were developed to prevent tripping of non faulted phases during fault in this period. It was shown that there will be some CT error which will lead to a quicker decay rate for the DC component on the secondary side of the CT. This made it necessary to propose a method that was not dependent on the DC component present on the secondary side of the CT. A formula for calculating the time it takes for the current to cross zero the first time during zero-miss was chosen as base for the implementation. Due to limitations in the Digsi software, the logarithmic function and cosine function had to be approximated.

It was proven in chapter 7 that the approximation made in order to implement the formula for calculating time to zero-crossing was accurate. Preliminary testing show that tripping of faulted phase can be done without tripping of healthy phases during zero miss. Further testing is however recommended.

Future work As future work, this report recommends the following:

- Test the implementation in a SIPROTEC relay with 1 pole tripping as a standard option
- Conduct an investigation regarding ferroresonance due to the unbalanced loading in the period between tripping the faulted phase and the remaining healthy ones
- Investigate the level of accuracy that the actual current transformers can replicate the decaying DC component

- Measure the time constant of the system under normal loading to asses the error associated with using the $\frac{L}{R}$ ratio of the shunt reactor
- Investigate the process of measuring the switching angle θ during energization of the cable

Bibliography

[1] Silec Cabel. Cable Technincal Spesification 14-11-11

[2] F. Faria Da Silva, C. L. Bak, U. S. Gudmundsdottir, W. Wiechowski and M. R. Knardrupgård. Methods to Minimize Zero-Missing Phenomena

[3] GE Power Systems Energy Consulting, "Connecticut Cable Transient and Harmonics Study for Phase 2: Final Report", November 2003

[4] Filipe Miguel Faria da Silva. Analysis and simulation of electromagnetic transients in HVAC cable transmission grids.

[5] Filipe Faria da Silva, Claus Leth Bak. Electromagnetic Transients in Power Cables. ISBN 978-1-4471-5235-4

[6] Teruo Ohno. Dynamic Study on the 400 kV 60 km Kyndbyværket Ð Asnæsværket Line

[7] S. Sivanagaraju, S. Satyanarayana. Electric Power Transmission and Distribution. ISBN 978-81-317-0791-3

[8] U. A. Bakshi, M. V. Bakshi, Electrical Power Transmission and Distribution. 1 edition 2007

[9] Demetrios A. Tziouvaras. Protection of High-Voltage Cables, Schweitzer Engineering Laboratories, Inc.

[10] Ahmed Abu-Siada. Lecture 8 Underground Cables. Elecric Power Transmission and Distribution 604

[11] Alstom Grid. Network Protection and automation Guide, protective relays, measurement and control. edition may 2011.ISBN 978-0-9568678-0-3

[12] Merz-Price Protective Gear. K. Faye-Hansen and G. Harlow. IEE Proceedings, 1911

[13] Gerhard Ziegler. Numerical Differential Protection, Principles and Applications 2nd edition.

[14] Behrouz Ghorbanian. Power System Protection 302. Curtin University of Technology

[15] Aberdare cables, driven by Powertech. Cables Facts and Figures

[16] IEEE standard C57.21 (2008). IEEE standard requirements, terminology, and test code for shunt reactors rated over 500 kVA, IEEE, New York

[17] B. Kasztenny (GE Multilin), I. Voloh, (GE Multilin), J.G. Hubertus (PSE and G). Applying Distance Protection to Cable Circuits. Protective Relay Engineers, 2004 57th Annual Conference for. IEEE

[18] Kasper Schultz Pedersen. Håndtering af Zeromiss i forbindelse med kabelanlægning af Indkiledalen. 14 mai 2013

[19] web:www.energinet.dk

[20] Live Tank Circuit Breakers, Application Guide. ABB

[21] Svein Tore Hagen, Kompendium i Høgspenningsteknikk 2010

[22] Live Tank Circuit Breakers, Buyers Guide. ABB

[23] web: www.energy.siemens.com

[24] ABB Afbryderhåndbog 1997

[25] Unnur Stella Gudmundsdottir, Per B. Holst. Solving zero-miss with cable energization at voltage peak, based on insulation coordination study results

[26] Gerhard Ziegler. Numerical Differential Protection 2ed. principle and application. Siemens

[27] S. Hassan, M. Vaziri, S. Vadhva. Review of Ferroresonance in Power Distribution Grids

[28] V. Valverde, G. Buigues, A. J. Mason, I Zamora, I. Albizu. Ferroresonant Configurations in Power Systems

[29] Allan Greenwood, Electrical Transients in Power Systems. 1991

[30] Ph. Ferracci. Cahier technique no 190. Ferroresonance. Schneider Electric

[31] Unnur Stella Gudmundsdottir, Modelling of long High Voltage AC cables in Transmission systems.

[32] EMTP Reference Models for Transmission Line Relay Testing. Final-9/9 2005

[33] Muhamed Zalani Daud. Transient behavior modeling of Underground high voltage cable systems, University of Wollongong Thesis Collection 2009

[34] J, R, Lucas. High Voltage Engineering. 2001

[35] Osama Elsayed Gouda, Adel Abd-eltwab Farag. Factors affecting the sheath losses in single-core underground power cables with two-point bonding method.

[36] C.F Jensen, F. Faria da Silva, C.L Bak and W.Wiechowski. Switching studies for the Horns Rev 2 wind farm main cable

[37] Test report Serial No 8720809. Test Engineer Linus Jern. 2013-04-18 ABB AB Power transformers, Ludvika Sweden

[38] Stinger, Norman T. The Effect of DC Current Offset on Current-Operated Relays

[39] Holst, S. Zakonsek, J. Transient Behavior of Conventional Transformers used as Primary Transducers and Input Elements in Protection IED's and Stand Alone Merging Units.

[40] Holst, S. Bapuji S. Palki. Co-ordination of fast numerical relays and current transformers- over dimensioning factors and influence parameter.

[41] R. C: Gupta. Bhaskara I's approximate to sine. Birla Institute of Technology, Ranchi. 1967

[42] Thomas' Calculus. Including second order differential equations. Pearson education inc. 2005

[43] SIPROTEC, Distance Protection 7SA6xx V4 manual

Appendix A

Test setup

The test setup consists of a Omicron CMC 356 connected to a computer with the software Omicron Test Universe V2.40 SR1. The Omicron powers the SIPROTEC 4 7SA610 relay and also provides the input current. The relay is also connected to a computer with Digsi V4.89. The setup is shown in figure A.1

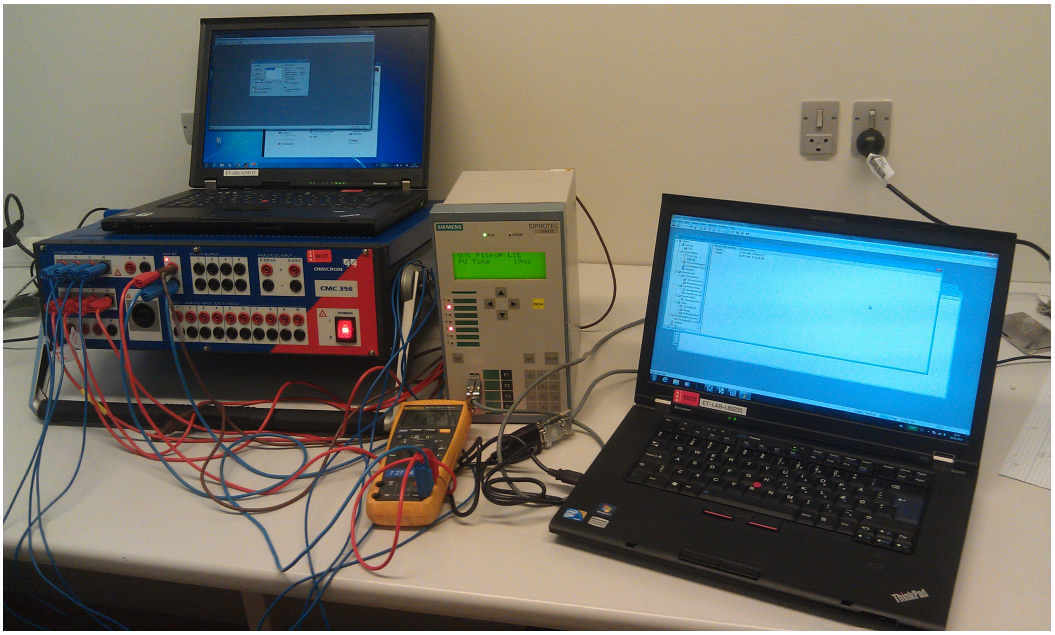

Figure A.1: Picture of the test setup

Appendix B

Ferroresonance

Ferroresonance includes all the oscillatory phenomenas that takes place in an electric circuit with a nonlinear inductance, a capacitance, low losses and a voltage source [30]. It is this oscillatory phenomenon caused by the interaction of the system capacitance with the nonlinear inductance of a transformer that is referred to as ferroresonance [27]. Ferroresonance can occur if a transformer and a cable becomes isolated and the capacitance of the cable is in series with the magnetizing characteristics of the transformer [5]. Ferroresonance is capable of creating sustained overvoltages with peak magnitude exceeding twice the rated peak voltage [27].

As mentioned, ferroresonance phenomenon is associated with the coexistence of a nonlinear inductance and a capacitance in the same circuit, connected either in parallel or series. The nonlinear inductance can in this case mainly be provided by a power transformer or a voltage transformer were the nonlinear characteristics are provided by saturation. The phenomena of ferroresonance is characterized by showing at least two steady state operating points,a non-ferroresonant and a ferroresonant [28]. The response of the ferroresonant circuit can jump from one stable point to another with sudden variations of current and voltage. ferroresonance can be divided into four different types: [30] [27]

- Fundamental mode: periodic oscillation at the fundament frequency.
- Sub-harmonic mode: periodic oscillation at sub-multiples of the fundamental frequency.
- Quasi-periodic mode: non-periodic oscillations with a discontinuous frequency spectrum.
- Chaotic mode: non-periodic oscillations with a continuous frequency spectrum.